(2)

NAVAL POSTGRADUATE SCHOOL
Monterey, California

THESIS

ARCJET PLUME IONIZATION EFFECTS ON EXPOSED SOLAR ARRAY CONDUCTING SURFACES

by

Richard W. Evert

September, 1991

Thesis Advisor: Dr. Richard C. Olsen

REPORT DOCUMENTATION PAGE

Form Approved
OMB No. 0704-0188

1a. REPORT SECURITY CLASSIFICATION Unclassified	1b. RESTRICTIVE MARKINGS
2a SECURITY CLASSIFICATION AUTHORITY	3. DISTRIBUTION/AVAILABILITY OF REPORT Approved for public release; distribution is unlimited.
2b. DECLASSIFICATION/DOWNGRADING SCHEDULE	
4. PERFORMING ORGANIZATION REPORT NUMBER(S)	5. MONITORING ORGANIZATION REPORT NUMBER(S)
6a. NAME OF PERFORMING ORGANIZATION Naval Postgraduate School 6b. OFFICE SYMBOL	7a. NAME OF MONITORING ORGANIZATION Naval Postgraduate School
6c. ADDRESS (City, State, and ZIP Code) Monterey, CA 93943-5000	7b. ADDRESS (City, State, and ZIP Code) Monterey, CA 93943-5000
8a. NAME OF FUNDING/SPONSORING ORGANIZATION 8b OFFICE SYMBOL	9 PROCUREMENT INSTRUMENT IDENTIFICATION NUMBER
8c. ADDRESS (City, State, ZIP Code)	10 SOURCE OF FUNDING NUMBERS PROGRAM ELEMENT NO. / PROJECT NO. / TASK NO. / WORK UNIT ACCESSION NO.

11. TITLE (Include Security Classification) ARCJET PLUME IONIZATION EFFECTS ON EXPOSED SOLAR ARRAY CONDUCTING SURFACES

12 PERSONAL AUTHOR(S) Evert, Richard W.

13a TYPE OF REPORT	13b TIME COVERED	14. DATE OF REPORT (Yr., Mo., Day)	15. PAGE COUNT
Master's Thesis	FROM_____ TO____	September 1991	72

16 SUPPLEMENTARY NOTATION
The views expressed in this thesis are those of the author and do not reflect the official policy or position of the Department of Defense or the U.S. Government.

17 COSATI CODES			18. SUBJECT TERMS (Continue on reverse if necessary and identify by block number)
FIELD	GROUP	SUB-GROUP	Arcjet, Electrothermal propulsion.

19. ABSTRACT (Continue on reverse if necessary and identify by block number)

High efficiency arcjet propulsion will be used in the near future for satellite orbit adjustment and eventually for orbit transfer. Testing is currently being conducted to explore spacecraft interface difficulties with this method of propulsion. This thesis looks at one aspect of this interface. Since most earth orbiting spacecraft use solar arrays for power generation, it is of interest to investigate how exposed, biased conducting surfaces will interact with the slightly ionized plume environment of the arcjet thruster. It was found that with the arcjet thruster mounted 25.4 cm above the solar array, firing along its axis at a 20 degree cant angle, electrical currents were indeed collected. The effect of having a constricted area exposed to the plume was to increase the current density. The electron densities at typical solar array distances were found to be 10^{10}-$10^{12}/m^3$. An estimate of the total power lost for an array in this configuration showed that 0.05% of the overall power is lost due to collected currents.

20 DISTRIBUTION/AVAILABILITY OF ABSTRACT ☒UNCLASSIFIED/UNLIMITED ☐SAME AS RPT. ☐DTIC USERS	21 ABSTRACT SECURITY CLASSIFICATION Unclassified

22a. NAME OF RESPONSIBLE INDIVIDUAL	22b TELEPHONE (Area Code)	22c OFFICE SYMBOL
R. C. Olsen	(408) 646-2019	PH/Os

Approved for public release; distribution is unlimited.

Arejet Plume Ionization Effects on Exposed
Solar Array Conducting Surfaces

by

Richard William Evert
Lieutenant, United States Navy
B.S., University of Southern California, 1984

Submitted in partial fulfillment
of the requirements for the degree of

MASTER OF SCIENCE IN PHYSICS

from the

NAVAL POSTGRADUATE SCHOOL
September 1991

Author: Richard W. Evert

Approved by: Richard C. Olsen, Thesis Advisor

Oscar Biblarz, Second Reader

Karlheinz E. Woehler, Chairman, Department of Physics

ABSTRACT

High-efficiency arcjet propulsion will be used in the near future for satellite orbit adjustment and eventually for orbit transfer. Testing is currently being conducted to explore spacecraft interface difficulties with this method of propulsion. This thesis looks at one aspect of this interface. Since most earth orbiting spacecraft use solar arrays for power generation, it is of interest to investigate how exposed, biased conducting surfaces will interact with the slightly ionized plume environment of the arcjet thruster. It was found that with the arcjet thruster mounted 25.4 cm above the solar array, firing along its axis at a 20 degree cant angle, electrical currents were indeed collected. The effect of having a constricted area exposed to the plume was to increase the current density. The electron densities at typical solar array distances were found to be 10^{10}-10^{12} /m^3. An estimate of the total power lost for an array in this configuration showed that 0.05% of the overall power is lost due to collected currents.

TABLE OF CONTENTS

ACKNOWLEDGEMENTS

I would like to thank all the people at TRW whose help and guidance was instrumental to this experiment. A special thank you to Sidney Zafran who made this experimental opportunity possible in the first place. Thank you also goes to Jaime Valles whose effort and time on this experiment were greatly appreciated. His insight and experience were key to overcoming several hurdles. Charlie Vaughn of Rocket Research Company helped in many ways with background information on the arcjet and the specifics of its operation. Very special thanks go to Professor Olsen for his guidance and time given to producing this thesis.

I. INTRODUCTION

A. ARCJET THRUSTER USE

Propulsion technology has advanced so that many electrothermal propulsion systems have become attractive operational alternatives to the usual auxiliary chemical thruster system. The efficiency of these electrothermal systems is much higher than their chemical counterparts allowing for a larger payload. One of these electrothermal devices is the arcjet thruster. The principle of operation for the arcjet involves the heating of a propellant within a high temperature arc discharge and its subsequent expansion through a nozzle to produce thrust. Current systems under testing are up to 2 kW power and have 450-600 second specific impulse and 0.13-0.44 Newton thrust. This type of thruster is excellent for station keeping purposes. Systems in the 3 kW to 10 kW power range will be useful for orbit transfer. Investigation of the effects arcjet thrusters have on other spacecraft systems has been ongoing and intensifying as deployment on spacecraft nears. [Ref. 1]

B. SPACECRAFT INTEGRATION

For thrusters that will be used for station keeping purposes the main system integration question is, how will the arc electromagnetic interference affect communications and other satellite systems? But as systems of higher power are

considered other potential spacecraft integration problems become of great concern also. Effects that the arcjet thruster may have on exposed solar array conducting surfaces is of particular interest. The exhaust plume of the arcjet is a partially ionized gas that may generate conduction paths to ground for the solar arrays thus reducing their power generation efficiency. Arcjets used for orbit transfer would require significant power, operating for long periods of up to several months. This implies that it is important to take a close look at arcjet plume effects on solar arrays.

The opportunity to do so arose during a spacecraft integrated test firing of a 1.4 kW arcjet on an operational qualification model communications satellite in a vacuum environment (1.2×10^{-3} Pa) at TRW in Redondo Beach, CA. Exposed conducting surfaces (with areas typical of solar array connectors and junctions) were placed in various positions on the solar panel. These surfaces were biased to varying voltages, and the current measured to determine losses due to ionized plume conduction. Additional conducting surfaces having larger areas were also used in order to estimate the plasma character at these positions.

C. THESIS ORGANIZATION

This thesis will describe the arcjet thruster operating principles and discuss the interaction principles governing the processes being investigated. This will be followed by a description of the experiment and the results obtained. Finally conclusions and follow on areas of investigation will be presented.

II. ELECTROTHERMAL PROPULSION PRINCIPLES

Electrothermal propulsion is based on the same principles for propulsion as a chemical system where the gas is heated and expanded through a nozzle. However instead of chemical combustion providing the heat, heat is generated electrically. Electrothermal propulsion provides lower thrust than a chemical system, but the specific impulse can be much higher. Electrothermal systems are not suitable for launch, due to their low thrust. Their utility is in on orbit station keeping and maneuvering. Orbit transfer will be possible with bigger systems under development.

The higher specific impulse of electrothermal systems will allow them to perform the same mission as a chemical system using less total weight. The thruster and electrical power unit weight are comparable to the hardware of a chemical system but much less propellant is required. The first generation of electrothermal propulsion systems is the resistojet.

A. RESISTOJET THRUSTERS

The resistojet shown in Figure 1 below is a typical arrangement for this type of system. The thruster propellant is either nydrogen (H_2), nitrogen (N_2), ammonia (NH_3), or hydrazine (N_2H_4). The propellant is delivered into the gas generator chamber, via the catalyst bed in the case of hydrazine (the intended flight propellant). Here it is decomposed into nitrogen, hydrogen, and ammonia. Since

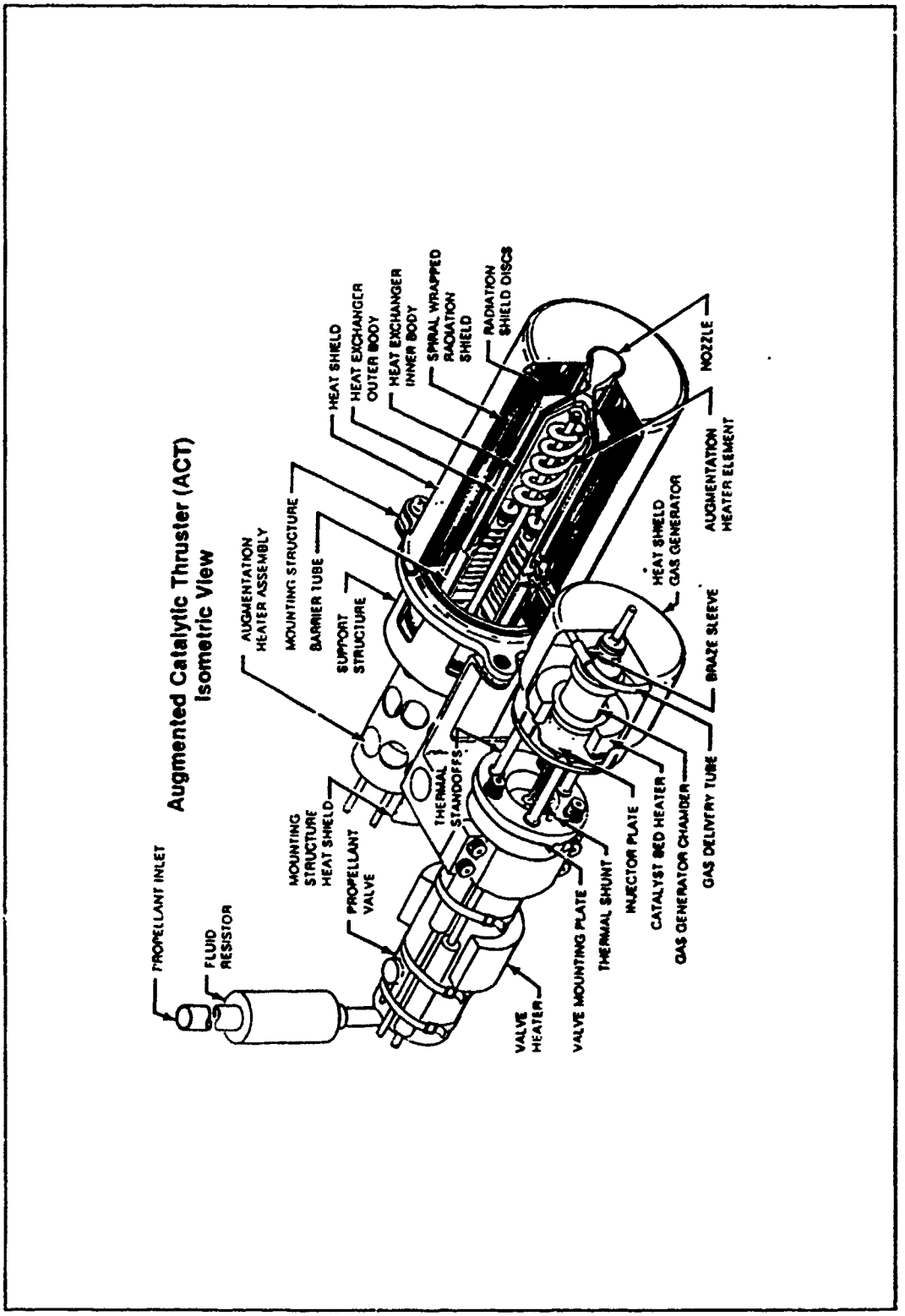

Figure 1 Resistojet [Ref. 1]

the decomposition reaction is exothermic, the propellant also gains heat at this stage. From the gas generator chamber the gas delivery tube transfers the propellant to the heat exchanger where the electrical heater element heats the gas prior to its entry into the nozzle.

Through the nozzle, the gas undergoes an adiabatic expansion to generate the thrust. This is identical to operation of a chemical thruster nozzle. The thrust generated is calculated from the temperature and other characteristics of the propellant gas at the entry to the nozzle. The efficiency of the system is very much dependent on the efficiency of the heat exchanger. In the resistojet the heat transfer occurs in a cavity around the augmentation heater.

This design has been used on SATCOM, GSTAR I-IV, and SPACENET I-IV satellites [Ref. 1]. The thruster used on these satellites operates on hydrazine propellant and provides a steady state thrust of 0.178-0.334 N thrust. The propellant flow rate range is 0.0590-0.127 g/sec. The mass of the arcjet thruster is 0.816 kg. [Ref. 1]

The SATCOM G and H satellites were launched in April and September of 1983, and SPACENET I and II were launched in May and November of 1984. As of August 1990 these resistojet thrusters have accumulated from 80 to 141 hours of burn time for station keeping. GSTAR III was launched in September 1988. It used resistojets for orbit transfer. GSTAR III has 180 hours of accumulated burn time [Ref. 1]. As of August 1990, a total of 20 satellites have been launched with resistojet thrusters for station keeping, with all firings nominal [Ref. 1].

The arcjet principles of operation are the same as those for the resistojet. However, the arcjet differs from the resistojet in the method of heat transfer, and this leads to some additional complications, especially concerning integration with other spacecraft systems.

B. ARCJET THRUSTER

In the arcjet thruster, the heat transfer to the propellant is accomplished by convection and conduction from a plasma arc. The significant configuration differences are shown in Figure 2.

Note the difference from the resistojet in that the nozzle is also functioning as the anode for the arc and the region of heat transfer is smaller. The arc is established between the cathode probe and nozzle/anode as shown in the lower portion of Figure 2. The gas is injected tangentially to the cathode in order to stabilize the arc, cool the walls and to increase the time for heat transfer from the arc to the gas. The power required for establishing and maintaining the arc is provided by the power conditioning unit (PCU).

The first operational use of the arcjet thruster is scheduled to be on the TELSTAR 4 satellite scheduled for launch in late 1993 [Ref. 1]. The arcjet thruster in this experiment is a prequalification, mature, engineering-development model of the thrusters planned for the TELSTAR 4 satellite. All significant engineering design aspects are the same as the flight model thruster.

Research on arcjets of varying designs and power levels was conducted in the

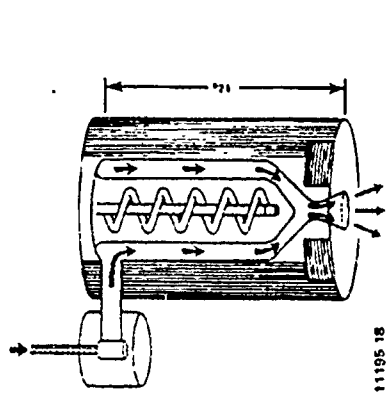

RESISTOJET HEAT TRANSFER REGION

- HEAT TRANSFER
  - RADIATION HEAT TRANSFER FROM HOT FILAMENT TO HEAT EXCHANGER WALLS
  - CONVECTION, CONDUCTION HEAT TRANSFER TO GAS
- ELEMENTS

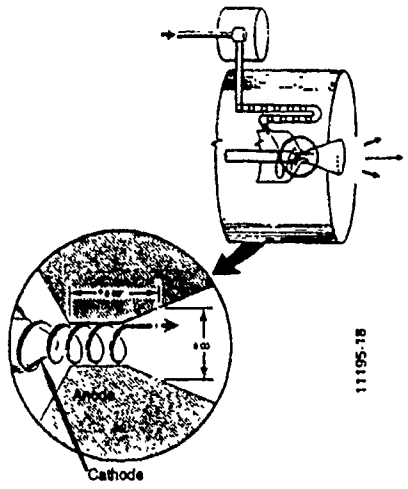

ARCJET HEAT TRANSFER REGION (ENLARGED TO SHOW DETAIL)

- HEAT TRANSFER
  - CONVECTION, CONDUCTION FROM PLASMA ARC REGION (>20,000 °K) TO GAS
  - GAS INJECTED TANGENTIALLY PROVIDES ARC STABILIZATION, KEEPS WALL COOL

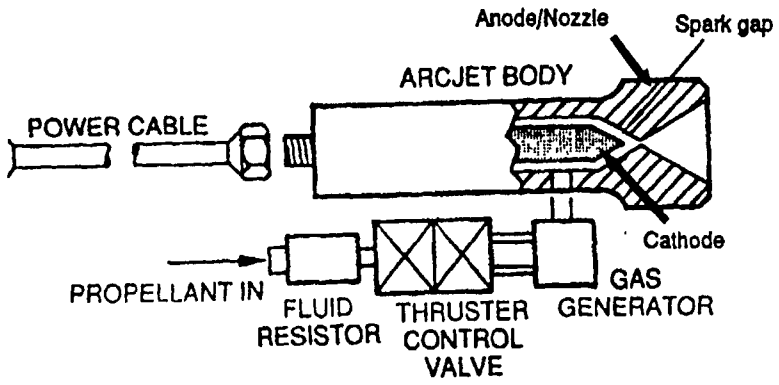

Figure 2 Arcjet / Resistojet Comparison [Ref. 1]

early 1960's [Refs. 2-4]. This work showed them to be a promising alternative to chemical systems although the thrust levels were lower than desired for the low power versions. Research was focused on magneto-plasma-dynamic (MPD) thrusters throughout the 70's and into the mid 80's [Ref. 5]. The MPD thruster differs from the arcjet thruster used in this experiment. The MPD arcjet is an evolution from the arcjet thruster that achieves much higher ionization of the propellant, and relies on electromagnetic forces for thrust rather than the thermal expansion through a nozzle. A survey of the literature in the Journal of Aeronautical and Astronautical Abstracts reveals that the field was devoted soleley to the MPD thruster design until 1985, when thermal arcjets came back under study.

Recent work on thermal arcjets includes studies of the plume characteristics (ionization, enthalpy, temperature, composition), and the design of the thruster anode (nozzle) and cathode [Refs. 6-8]. The recent studies are similar to earlier work with the focus now being on low power arcjets since they are near deployment.

The main concerns at this point are issues involving the integration of the arcjet to spacecraft. One concern is the electrical currents collected by the solar arrays from the ionized exhaust gas produced by the arcjet. The basic physics of this process is considered in the next chapter, along with a review of previous lab work on arcjet plasma characteristics.

III. PLASMA PRINCIPLES

A. PROBE THEORY

A solar array has exposed biased conducting surfaces. Immersed in a plasma, these surfaces will collect currents from that plasma. The interaction of biased surfaces in plasmas is explained well by Debye theory for small potentials. If the potential is on the order of or larger than the electron temperature, then these interactions become more complex. The theoretical development is quite complete for idealized spherical and cylindrical objects such as Langmuir probes [Refs. 9 and 10]. Assuming an infinite quasineutral plasma with a mean free path, λ, large compared to other system dimensions, a charged probe placed in a plasma will create a potential for the charged particles in the plasma and they will redistribute according to this potential and the probe geometry. This will result in a shielding out of the probe by attracted ions or electrons that form a sheath around the probe.

Figure 3 depicts this shielding out principle. There will be a spherical surface defined by $\phi = 0$ relative to the plasma potential. Outside of this surface the particles do not sense the charged spherical object.

The current density of the probe is given by

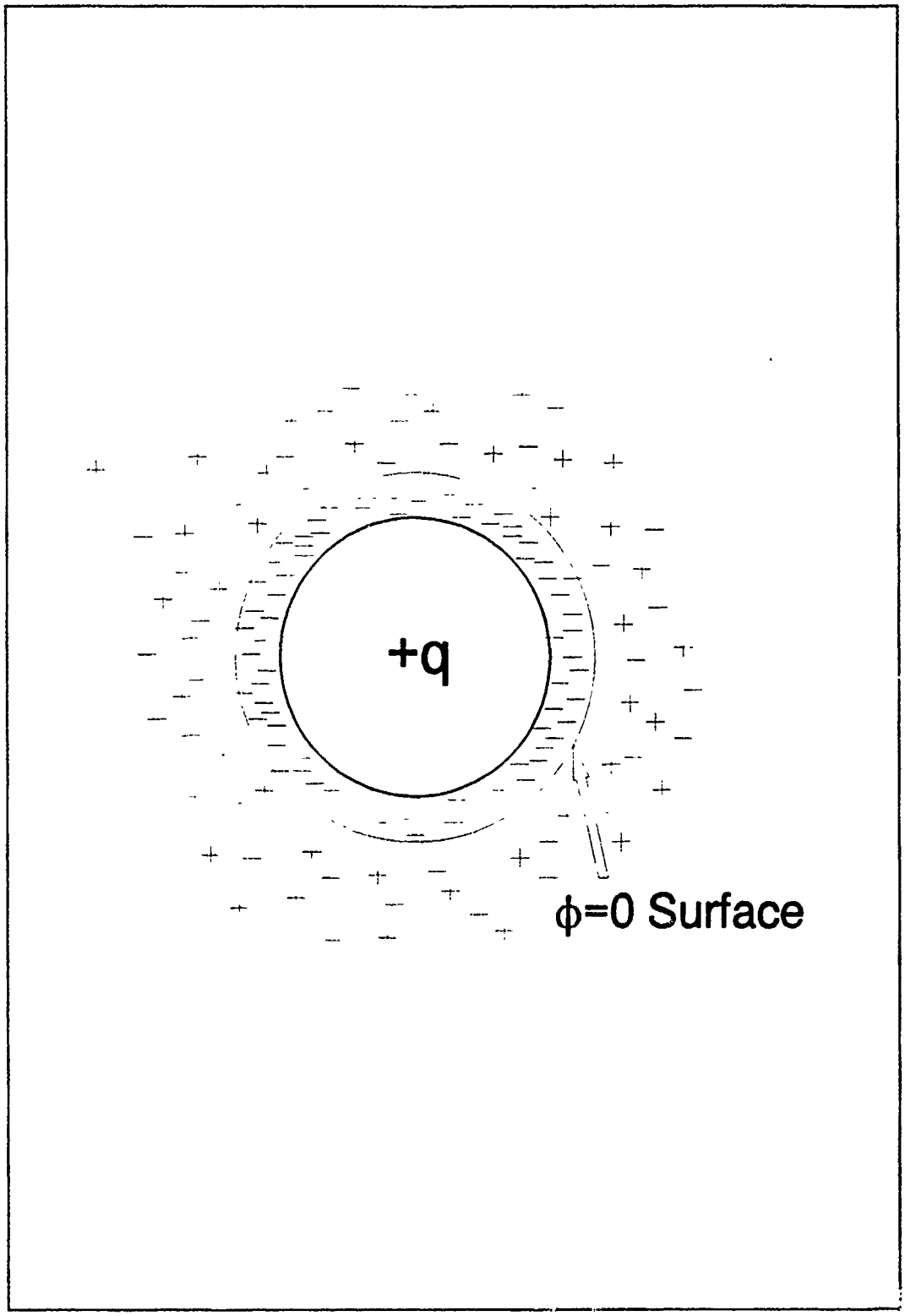

Figure 3 Debye Shielding of a Spherical Charged Object in a Plasma

$$J_s = \frac{1}{4} n_o q \bar{v}_s \tag{1}$$

where J_s is the current density, n_o is the ion or electron number density (by quasineutrality), q is the species charge in coulombs, and $\bar{v}_s$ is the mean species velocity [Ref. 9].

If the probe is spherical with radius r_p, and the absolute value of the potential $|\phi|$ of the probe is small compared to kT/e, then the sheath thickness around the probe will typically be small compared to r_p and will be on the order of a few Debye lengths, λ_D [Ref. 9]. This will also leave the bulk of the plasma undisturbed. If the charged particle species (electrons or ions) in this sheath are characterized by a Maxwell-Boltzman velocity distribution, then the current density would be the familiar

$$J = n_o q \left(\frac{kT}{2\pi m_{e,i}} \right)^{\frac{1}{2}} \exp\left(\frac{q\varphi}{kT} \right) \tag{2}$$

where k is the Boltzman constant, and m_s is the species' mass in kg [Ref. 9].

This familiar equation is used extensively with Langmuir probe investigations of plasmas [Ref. 9]. In the experiment documented by this thesis, the conductor is of planar geometry and is biased such that the sheath region is much different from Debye theory and thus will take on a character like that pictured in Figure 4. The plasma source (the arcjet thruster) is generating a maxwellian plasma from a small spot source which expands and is affected by the potential of the plate once electrons

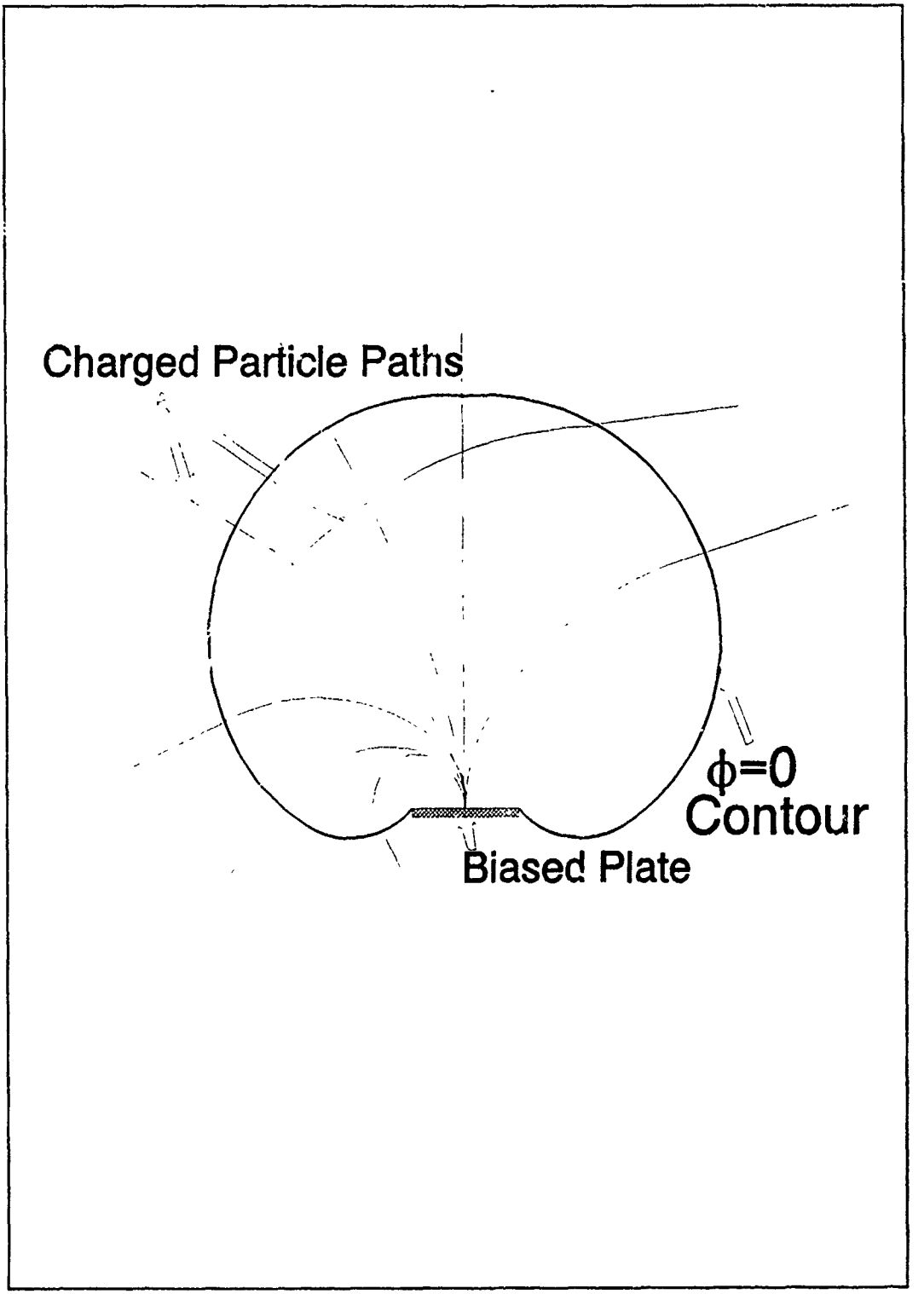

Figure 4 Plasma Charged Particle Interaction with an Oppositely Charged Plate with a Pinhole of Exposed Surface

or ions cross the $\phi=0$ potential surface.

The assumption that $e\phi$ is small compared to kT is not valid for this experiment. This is a basic assumption to obtain Equation 2 from Equation 1. Another assumption implicit in Equation 2 is that the conductor geometry is spherical. This will mean that the plate's potential will effect the bulk plasma and no precise information can be gained about the overall density of the plasma. Nevertheless Equation 1 holds for this experiment, so long as it is applied to the region near the plate. Therefore to obtain qualitative estimates of the electron density, $\bar{v}$ in Equation 1 will be determined from the assumption that the velocities of the charged particles in the sheath region are due to the potential of the conducting surface. This leads to a current density of

$$J=en_o\left(\frac{2q\varphi}{m_s}\right)^{\frac{1}{2}} \tag{3}$$

where $\bar{v}$ has been related to the potential by

$$\frac{1}{2}mv^2=q\varphi. \tag{4}$$

Equation 4 is just an expression of the conservation of energy and as long as the particles remain outside the $\phi=0$ contour then they are not in a potential field and their kinetic energy is just $\frac{1}{2}mv^2$. An approximate sketch of what is occurring as this applies to this experiment is in Figure 4. The charged plate creates a region of potential out to the $\phi=0$ contour where the plate potential is shielded out as

described above. The contour depicted is not necessarily representative of the actual surface but is intended to indicate further complexity beyond the simple spherical arrangement of Figure 3. With large λ, the particles will be traveling in random straight paths from the source of the plasma generation. As these particles cross the contour they are either repelled from or attracted to the plate. If their entry angle is appropriate, they will be collected on the plate. It is at the plate surface that the density n can be evaluated by Equation 3. We might expect that this density at the plate surface will vary with the density outside the sheath.

B. PREVIOUS ARCJET PLUME INVESTIGATIONS

Investigation of the arcjet plume has been of considerable interest as the details of spacecraft integration are being worked out. The plume has been investigated in the region very near the arcjet thruster exit plane (<35 cm) [Refs. 2, 6, 7, 11].

1. Arcjet Plume Ionization Investigations by Langmuir Probe

The plume characteristics of a low power (1.1 kW) dc arcjet have been investigated [Refs. 6, 11]. These studies were conducted using spherical and cylindrical Langmuir probes to determine plasma number density and temperature as a function of position in the plume and as a function of arcjet operating condition. The thruster propellant was a 2:1 ratio of hydrogen to nitrogen to simulate decomposed hydrazine. A vacuum tank pressure of 0.05 Pa was maintained. Two stationary probes were positioned at 30.5 cm down the plume axis with one probe on

the axis centerline and one 15.2 cm off centerline. A moveable probe was positioned 18.4 cm down the plume axis.

In these investigations the probe potentials were kept small relative to kT_e. Equation 2 applies and the electron density can be determined at plasma potential by

$$n_e = \frac{J}{e}\left(\frac{2\pi m_e}{kT_e}\right)^{1/2} \tag{5}$$

where the electron temperature is determined by the slope of the linear portion of the characteristic curve and knowing

$$\frac{d}{dV}(\ln I_e) = \frac{-e}{kT_e} \tag{6}$$

which is obtained by taking the logarithm of Equation 2 and differentiating with respect to the probe voltage. [Ref. 6, 11]

The I-V characteristics of the spherical probe at 30.5 cm on the plume centerline is shown in Figure 5. From this voltage versus current plot, using the slope of the linear portion of the curve, Equation 6 yields an electron density of $3.5 \times 10^9/cm^3$ [Ref. 11].

Figure 6 shows the electron number density found as a function of angle off centerline and the electron temperature as a function of the same angle. These measurements are for an axial distance of 18.4 cm. Note the exponential decay of the density and note that the density is half of the centerline value at 25° [Ref. 11].

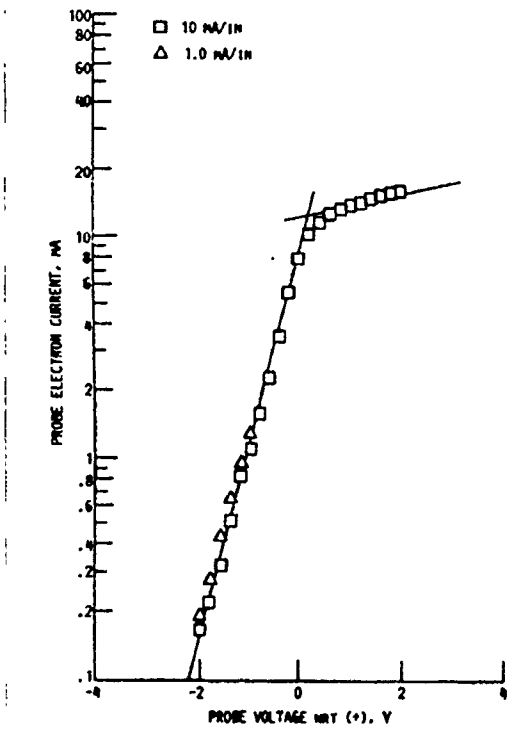

Figure 5 I-V Characteristic Graph of Arcjet Plume [Ref. 11]

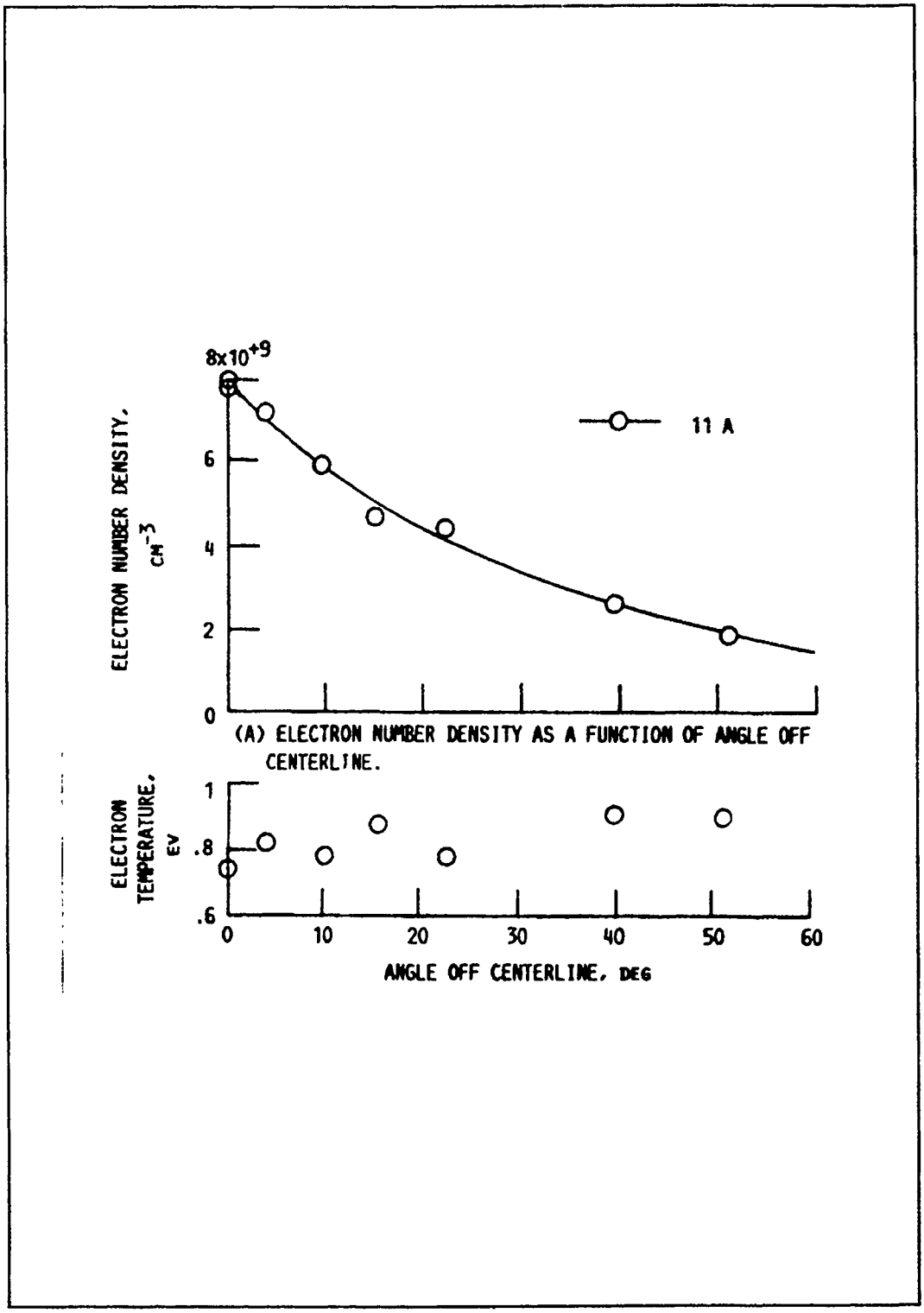

Figure 6 Electron Temperature and Density from Langmuir Probe Investigations as a Function of Angle Off Centerline [Ref. 11]

The value for electron temperature is 0.8 ±0.2 eV, and does not show variation with angle off centerline [Ref. 11]. This would be reperesentative of the case for large λ. The potentials used in this experiment vary from -200 to +200 volts and $q\phi >> kT$.

The measured electron number density as a function of distance along plume centerline is shown in Figure 7. The axial distance varies from 12 to 32 cm. Note the exponential decrease with distance. These studies discuss further investigations of the plume characteristics as a function of propellant mass flow rate and arcjet power, but the graphs presented are the subset of the data germane to this thesis. Carney's overall findings were that the plume ionization is less than one percent and that the plasma potential is very near facility ground. [Refs. 6, 11]

2. Plume Ionization Investigations by Spectral Emission

Arcjet performance and characteristics have been investigated by the use of spectroscopy [Refs. 2, 7]. Determining electron density by the method of spectroscopy relies on spectral line broadening due to the Stark effect. Stark broadening of the spectral lines

> ...produces Lorentzian line shapes and is caused by the interactions of the (spectral) emitters with charged particles. [Ref. 7]

The full width at half maximum broadening ($\Delta\lambda$) is related to the electron density by

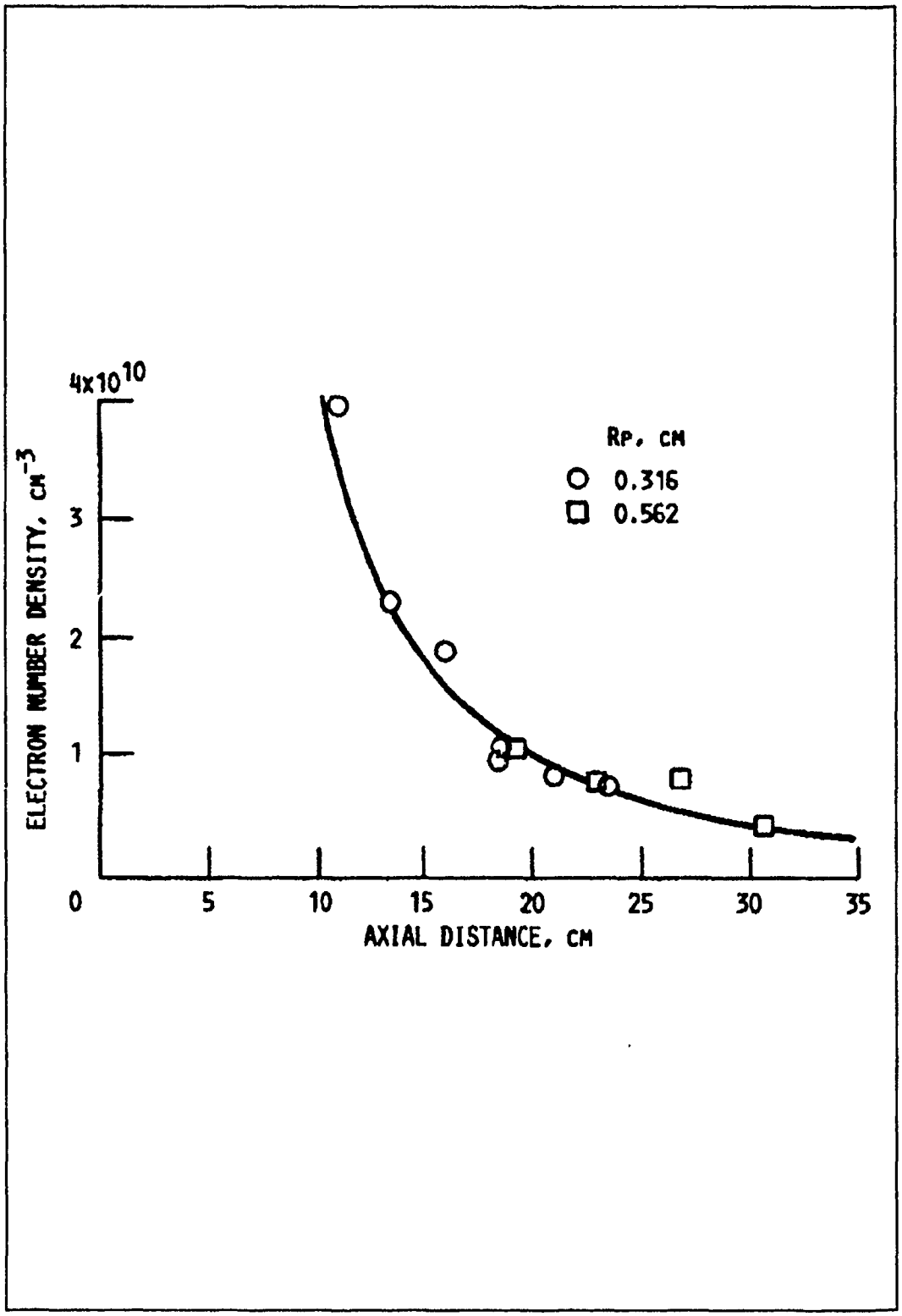

Figure 7 Electron Density vs. Axial Distance [Ref. 11]

$$\Delta\lambda_{1/2}\ (\text{Å}) = 2.5\times10^{-9}\,\alpha_{1/2}\,n_e^{2/3} \qquad (7)$$

where n_e is the electron density in cm^{-3} and $\alpha_{1/2}$ is the theoretical width at half maximum. This technique can be used on several different lines of the emission spectrum. [Refs. 7, 9]

The work by VanCamp and others included a study of plume electron density by Langmuir probe and spectral line broadening due to the Stark effect. Arcjets in a power range of 6 - 42 kW were studied. The propellant was hydrogen only. The electron density measurements presented in Figure 8 are for 30.3 kW (over 20 times the power of the arcjet involved in this experiment) and are determined by Langmuir probe 2 cm from the exit plane. The dip in electron density at the centerline is not reflected in any of the other more recent studies, but the overall electron density is in good agreement.

The graph in Figure 9 is the electron density as a function of arcjet power and were obtained by the method of line broadening due to the Stark effect [Ref. 2]. The densities are about five times that found by the Langmuir method in Figure 8. Due to techniques and technical difficulties the results presented are more qualitative than those in the previous study [Ref. 2].

The work by Manzella and others was conducted solely using spectroscopy on a 1 kW arcjet operating on a 2:1 hydrogen-nitrogen mixture [Ref. 7]. This investigation found an electron density of 1.8×10^{13} electrons/cm^3 on centerline in the exit plane. This was determined by a measured $\Delta\lambda$ in the H_β emission line of 0.34

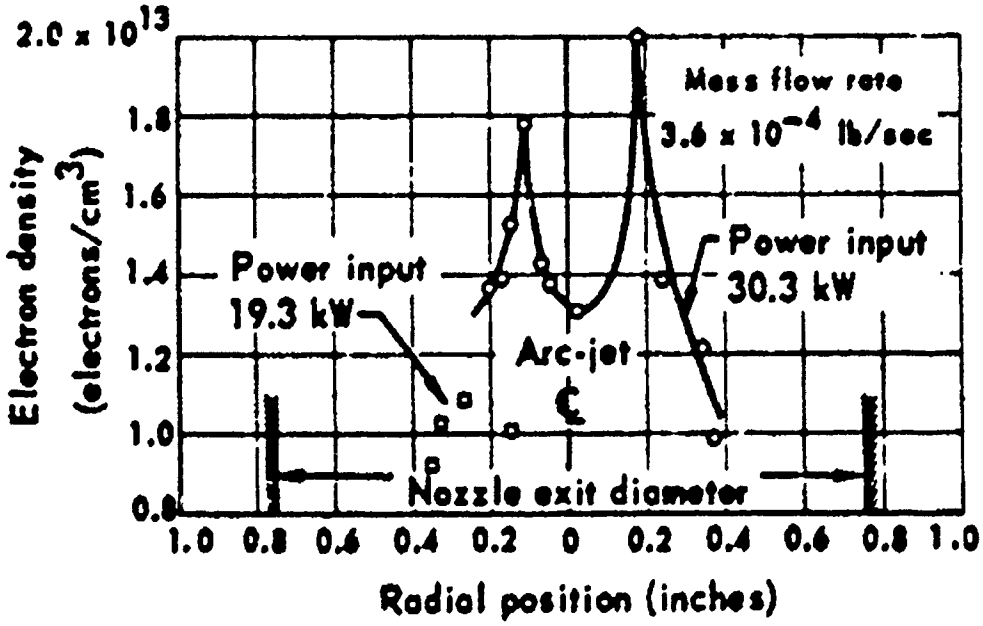

Figure 8 Electron Density Measurements [Ref.2]

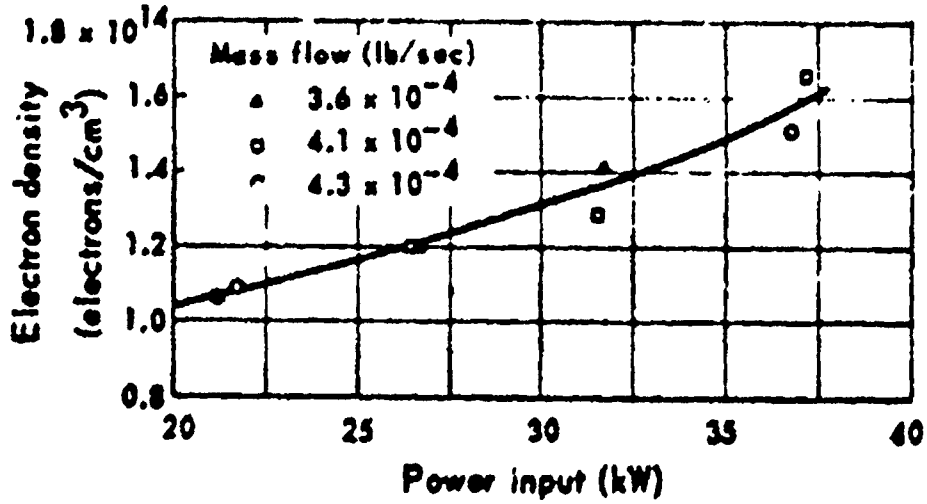

Figure 9 Electron Density Determined by the Stark Effect [Ref. 2]

Å. [Ref. 7]

C. SOME EXPECTATIONS

Based on the above studies, we can estimate some of the results from this experiment. Given that the plume is ionized to about 1%, this experiment should yield measurable currents [Refs. 6, 11]. With an electron density of $1 \times 10^{16} m^{-3}$ at 18 cm distance from the source as in Figure 7 and assuming that the plasma density falls off as a function of $1/r^3$ and that at an angle of 20° off of centerline the density is roughly half of the centerline value as in Figure 6, then we would expect densities of $4 \times 10^{12}/m^3$ to within 1 order of magnitude. If the mean free path is large, then there will be little exchange of energy and we can expect the electron temperatures to remain 0.8 ± 0.2 eV over all distances in the vacuum chamber [Ref. 11].

IV. EXPERIMENT DESCRIPTION

A. EXPERIMENT OVERVIEW

The arcjet test firing at TRW that provided the opportunity to look at the arcjet plume/biased surface interaction is part of the Arcjet System Integration Development (ASID) program. The objectives of this ASID program are to investigate electromagnetic interference (EMI) and plume impingement. These objectives were accomplished by operating the arcjet in a vacuum environment near the powered FLTSATCOM satellite [Ref. 12] by:

- Measuring EMI coupled into the spacecraft.
- Measuring EMI radiated with antennas.
- Measuring plume characteristics with radiometers, calorimeters, and witness plates positioned in various stations.

Along with these test goals, the interaction of the ionized plume with exposed biased conducting surfaces was investigated. As the arcjet was operating, the solar cell emulators and reference plates were biased to various voltages between -200 and +200 volts and the current was measured.

B. HARDWARE

The principle hardware in the test firing was the vacuum test facility, the arcjet system, the emulators and reference plates, and the measuring equipment.

1. Vacuum Chamber

The vacuum chamber is a 30 foot diameter sphere. It has four cryogenic vacuum pumps rated at 25,000 liters/second for H_2 or N_2 [Ref. 11]. In order to achieve and maintain chamber pressures of 10^{-3} Pa, the chamber also has a liquid nitrogen cooled inner wall and liquid helium cooled cryopumping array. When fully operating the chamber can pump 7.5×10^6 liters/second for H_2 or 3.8×10^6 liters/second for N_2 [Ref. 12]. These gases are the principle propellant constituents of the arcjet.

2. Arcjet

The arcjet was a 1.4 kW thruster operating on hydrazine propellant. It consisted of three principle subsystems: the arcjet thruster, the power conditioning unit (PCU), and the interconnecting power cable between the thruster and the PCU. These items are shown in Figure 10 and Figure 11.

The PCU stepped up the spacecraft bus voltage to approximately 100 volts dc and regulated the arc current during operation. It also would provide a brief 4000 volt pulse to initiate the arc during arcjet start up. The power to the PCU was provided by a 28 volt dc power supply external to the chamber.

The power cable between PCU and thruster was triaxial with center conductor connected to the thruster cathode. The inner shield was connected to the thruster anode or nozzle and the outer shield was connected to chassis ground.

The arcjet thruster was made by Rocket Research Company under the NASA Lewis Research Center sponsored Arcjet Research and Technology Program.

Figure 10 Arcjet Subsystems [Ref.1]

Figure 11 Picture of Arcjet Thruster [Ref. 1]

It was rated to provide 0.169 to 0.200 Newton thrust with a specific impulse of 450 seconds. The thruster mass was 1.36 kilograms. The electrical power of the arcjet was rated at 1260 watts. [Ref. 12]

3. Solar Cell Emulators and Reference Plates

Diagrams of these test items are in Figure 12 and a picture of one plate is in Figure 13. The conducting surfaces of the emulators and reference plates were 0.25 mm thick stainless steel. The exposed area of the reference plates was 3.14 cm^2. The emulators were covered by a 0.20 mm thick cover glass with a nominal 1.5 mm diameter hole, exposing an area of approximately 1.77 mm^2. Emulator one was damaged prior to the main experiment so no data was gathered from that position. The actual areas were as follows: (1) damaged, (2) 1.59, (3) 2.27, and (4) 1.89 mm^2. Each plate was mounted on 9.5 mm thick plexiglass and attached to the solar panel with adhesive tape

4. Measuring Equipment

Kiethley 617 programmable electrometers were used to measure the collected currents. A Hewlett Packard 6448B dc power supply provided the bias and an HP 3455A digital voltmeter measured it.

C. LAYOUT OF EXPERIMENT

The arrangement of the equipment in the chamber is shown in Figure 14 and Figure 15. The emulator plates were placed along the length of the solar array panel parallel to the arcjet thruster axis 42.5 cm off the axis center line. The reference

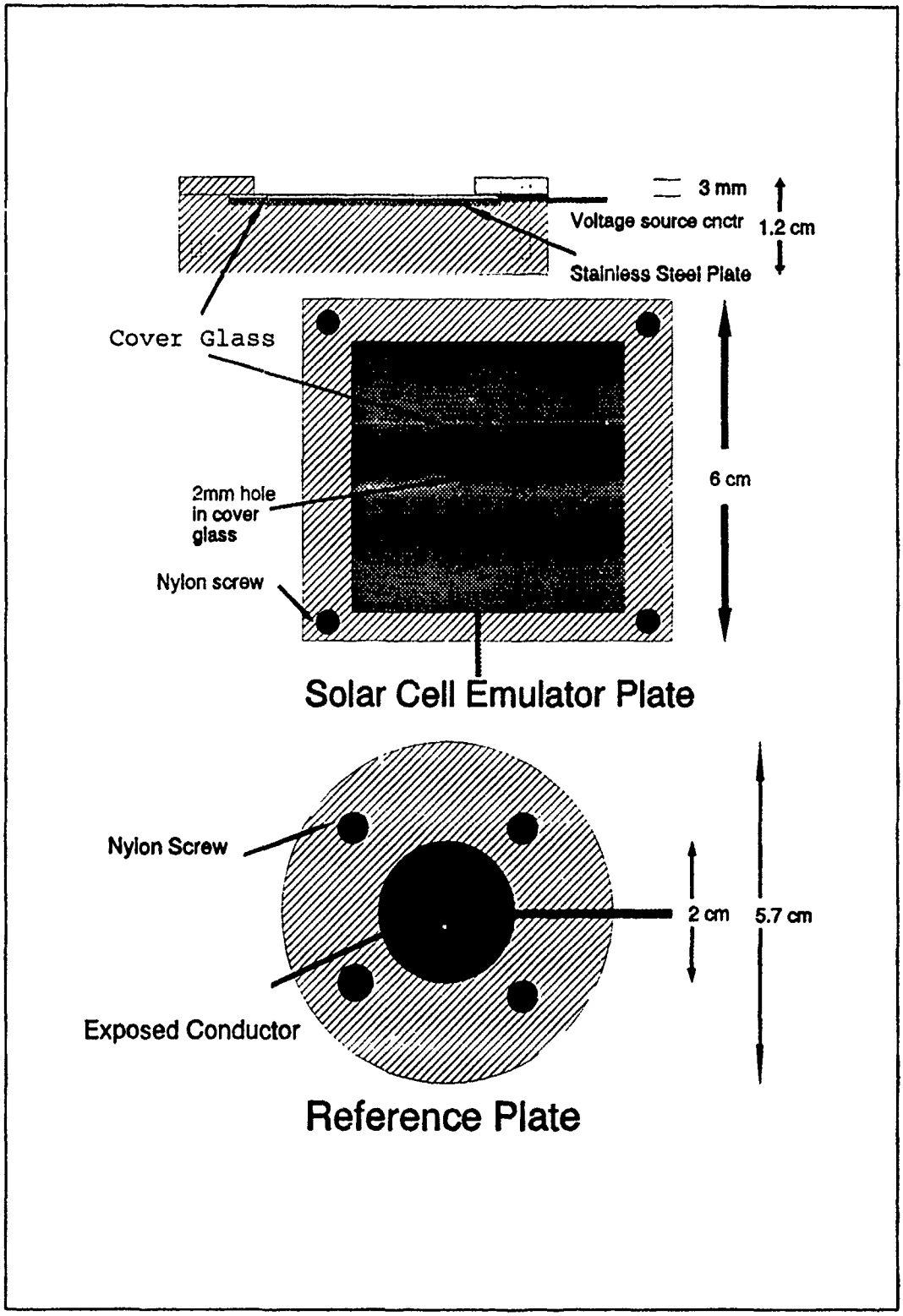

Figure 12 Diagram of Reference and Emulator Plates

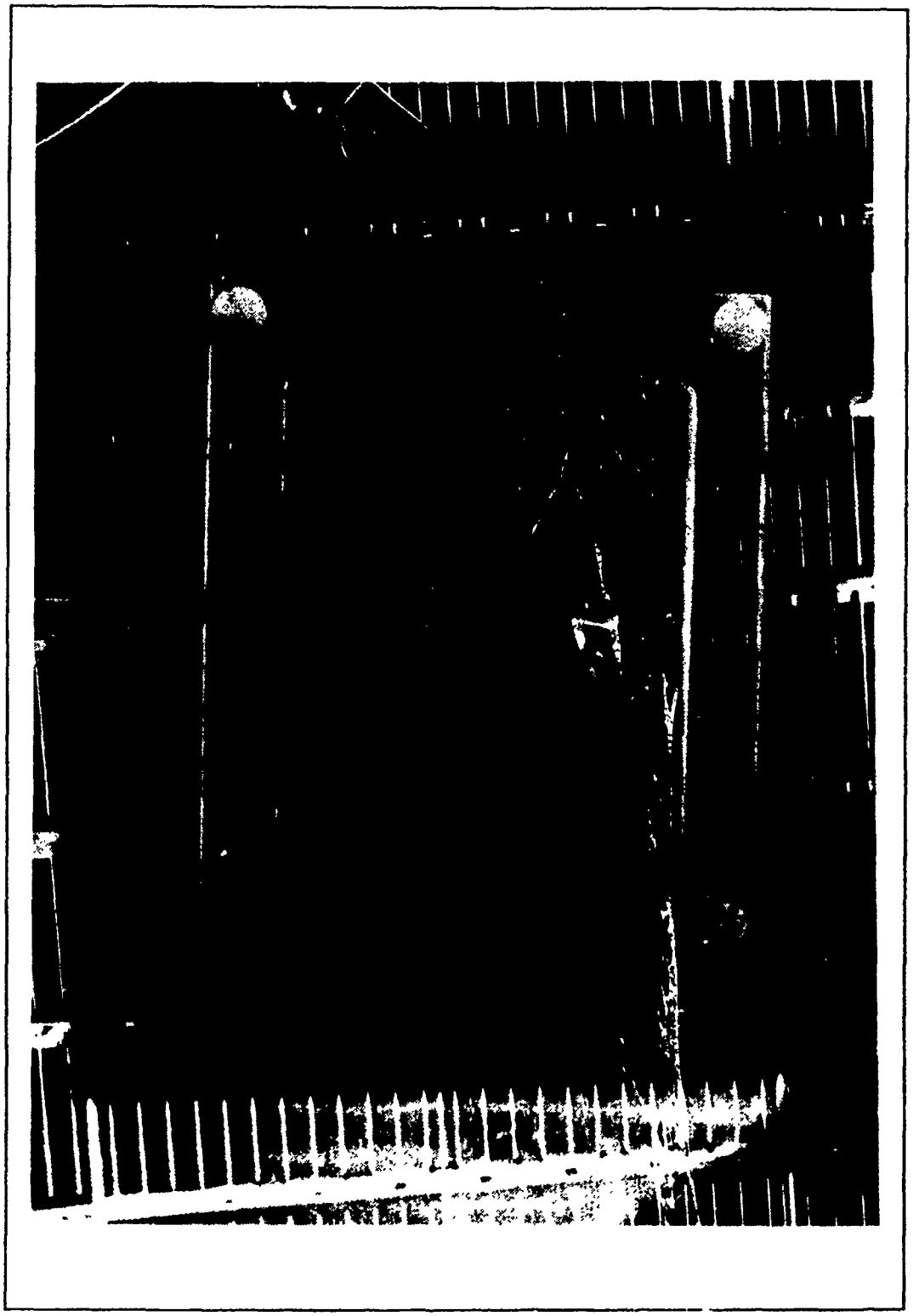

Figure 13 Picture of Emulator Plate

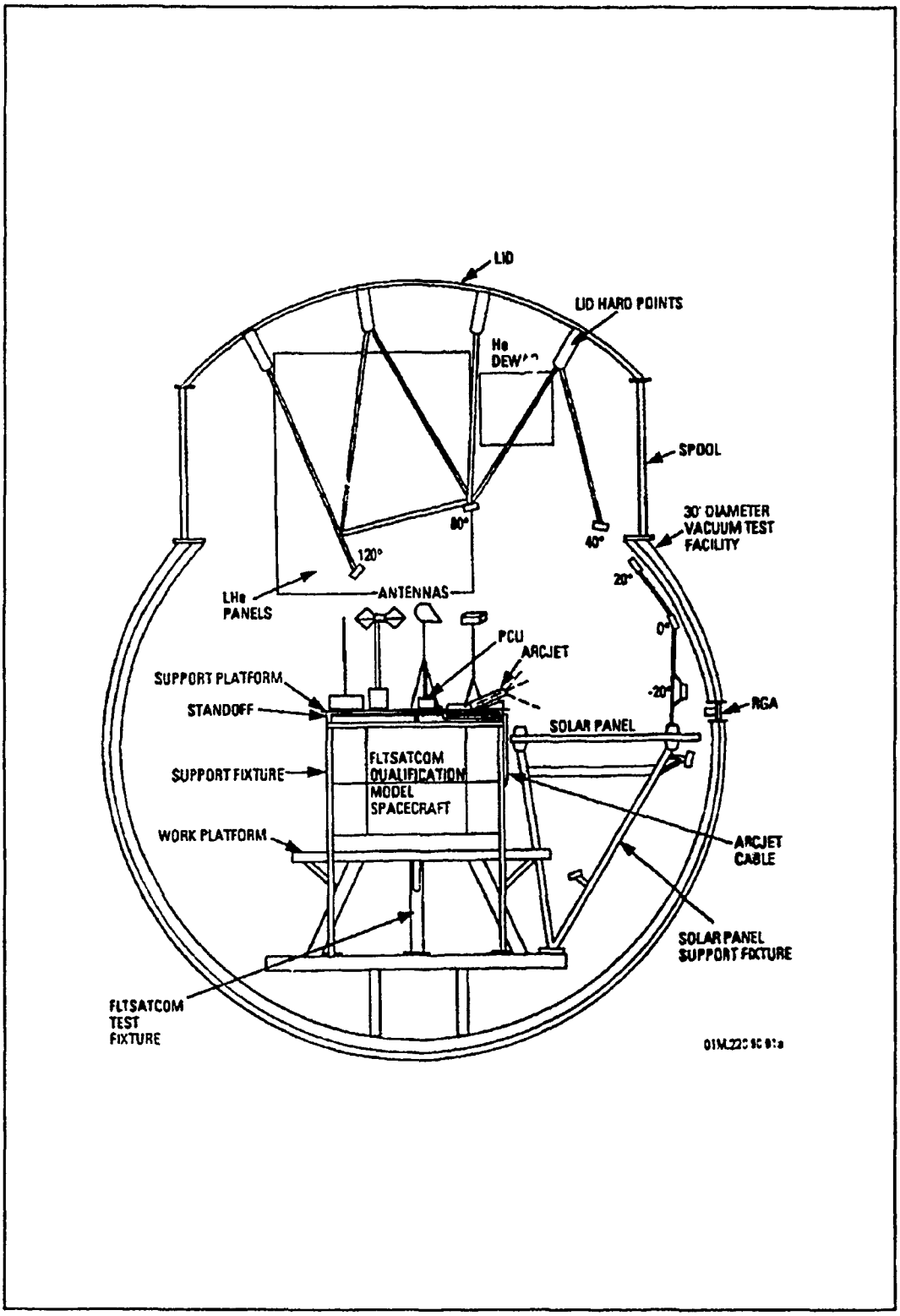

Figure 14 Vacuum Chamber Configuration Side View [Ref. 12]

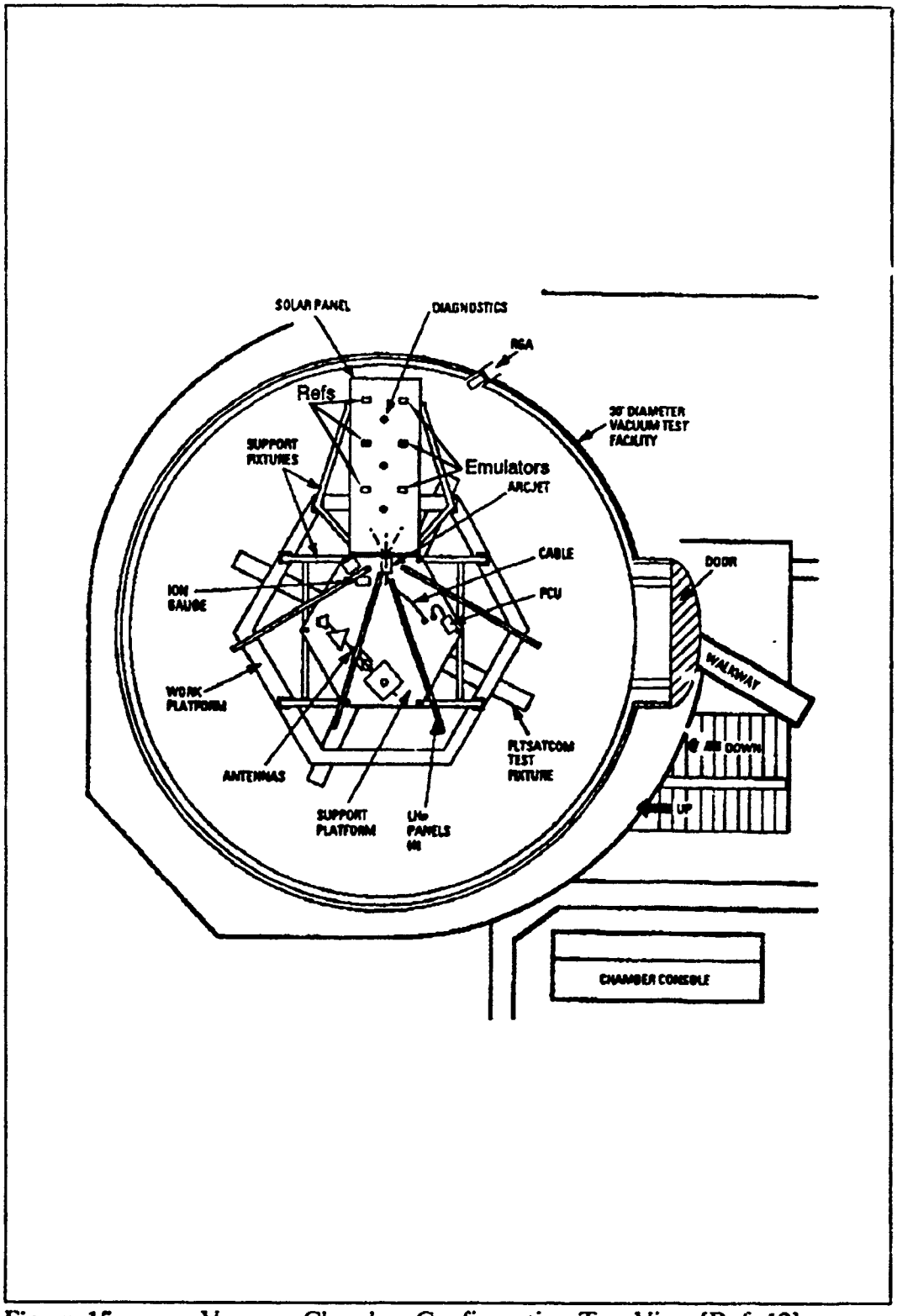

Figure 15 Vacuum Chamber Configuration Top View [Ref. 12]

plates were placed on the opposite side of the panel 36.2 cm off of the thruster axis centerline. The distances along the panel for both types of plates and the slant ranges from the arcjet nozzle are in Table 1.

TABLE I PLATE DISTANCES ALONG ARRAY PANEL AND SLANT RANGE TO ARCJET

	Emulators			References		
Plate #	E2	E3	E4	R2	R3	R4
Distance (cm)	104	165	259	104	165	259
Slant (cm)	115	172	263	113	171	263

The arcjet system was mounted to a support platform just above the satellite. The arcjet thruster was 25.4 cm above the solar panel centerline, canted 20° from the panel axis. This configuration is typical of geometries for north-south station keeping maneuvers [Ref. 12]. Figure 16 is a photograph of the chamber layout.

The plates were connected to the power supply and the measuring equipment via a connector in the wall of the chamber to a switching box. The diagram of this circuit is in Figure 17. Although the connector allowed for a floating ground, no noticeable difference in measurements of the two conditions was observed so the circuit was grounded to the common chamber ground.

D. PROCEDURE

Once the chamber pump down was complete a survey of line currents at voltages from -200 to +200 volts on the conducting plates was taken. No currents above 0.006 μA were measured at the extreme voltages, which established the

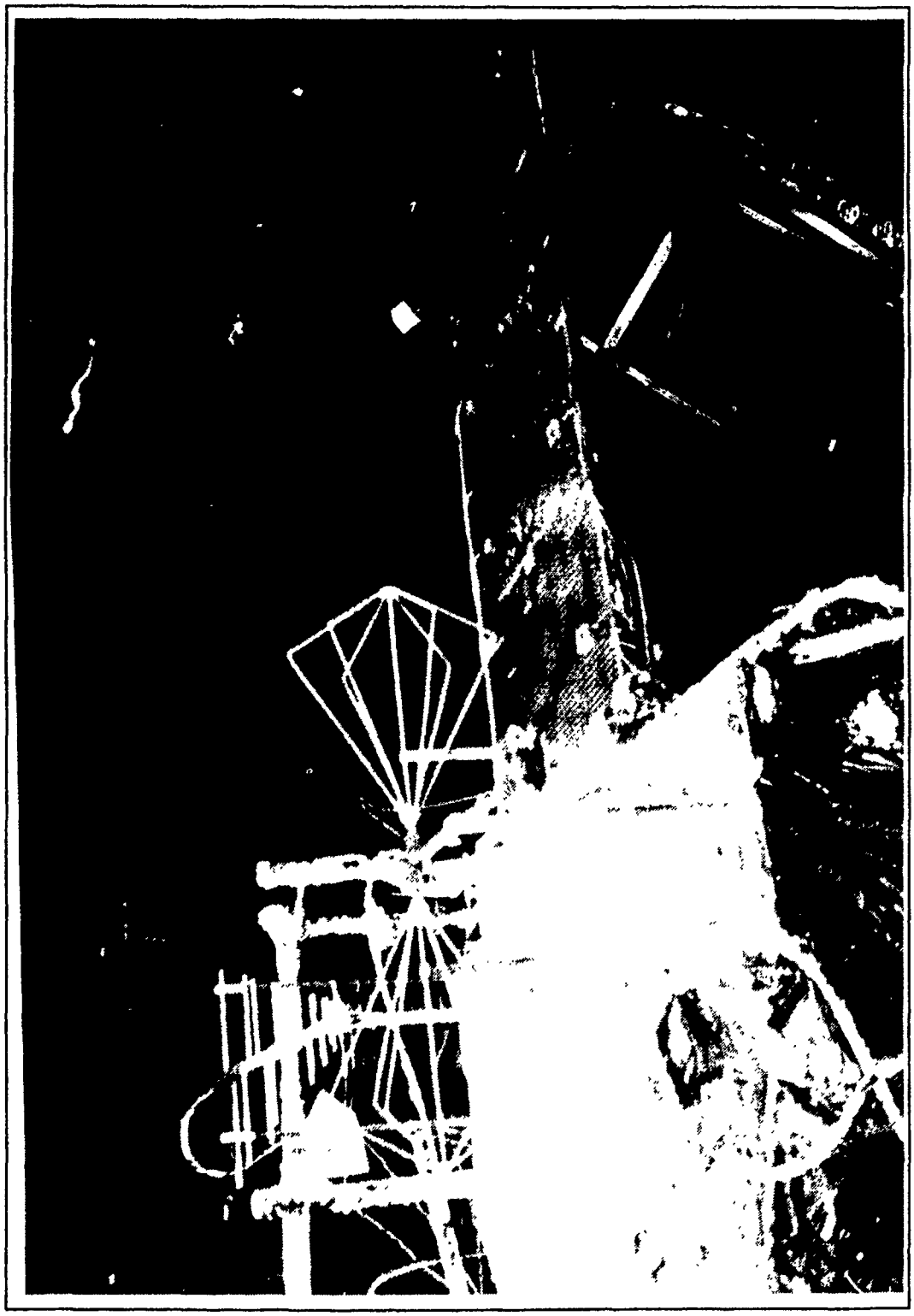

Figure 16 Picture of Chamber Ready for Firing Run

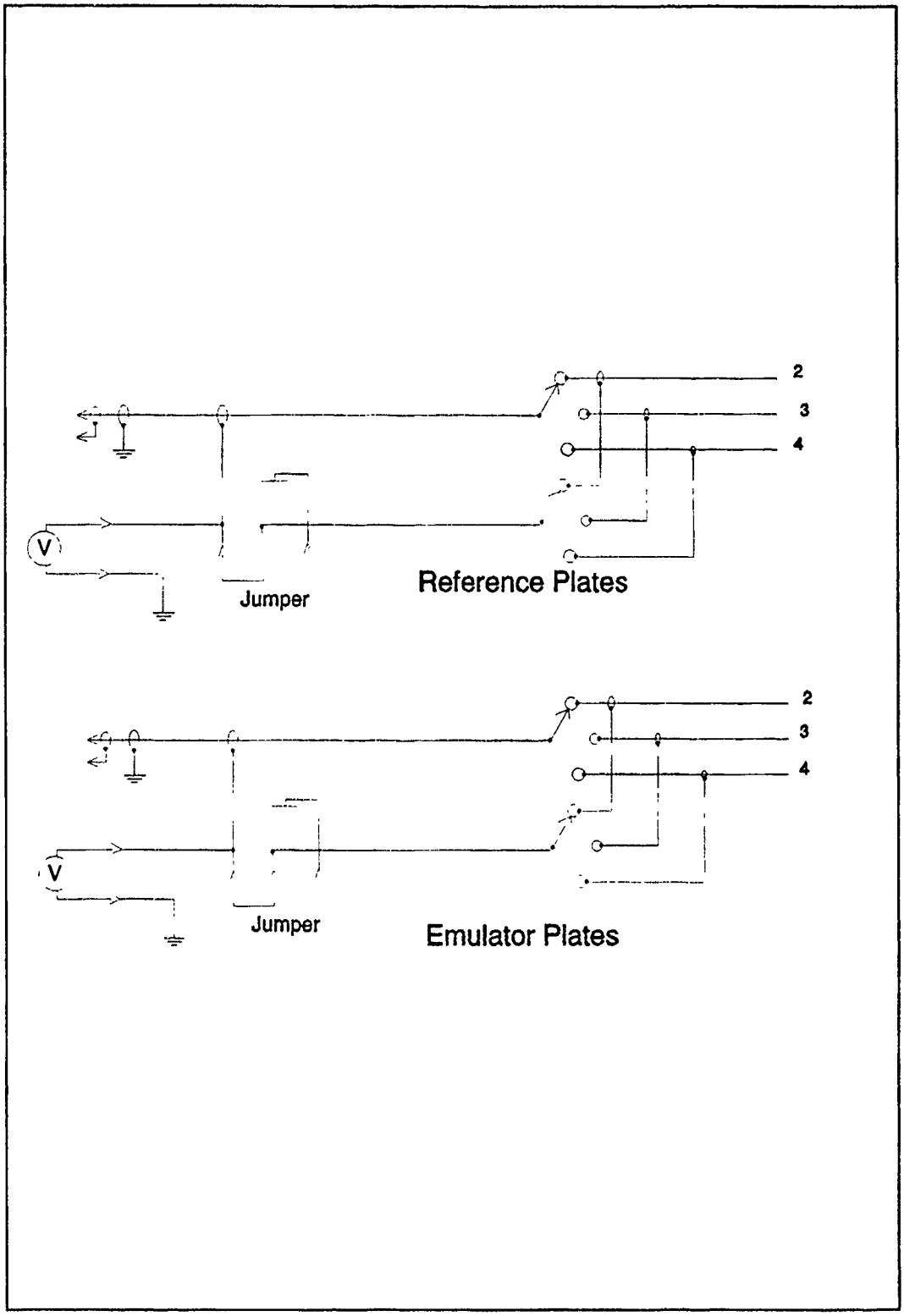

Figure 17 Schematic for Plate Biasing Circuit

baseline at less than 0.02% of any measured value in the arcjet environment. Once the arcjet was firing, the pressure on the chamber was maintained by the He panels, diffusion pumps, and N_2 shroud. Each plate was biased to varying voltages and current readings recorded.

1. Chronology

The first firing run was attempted on 24 July 1990. A pressure of 2.13×10^{-3} Pa was achieved. However freezing of the propellant in the propellant supply line prevented firing on this day. The following day the pressure had been brought up to 15.1 Pa and the propellant was no longer frozen in the line at this pressure. Rather than opening the chamber and attempting to fix the propellant line insulation immediately, the decision was made to do a firing run at the high pressure in order to collect some data in case a later attempt at a low pressure run was also unsuccessful. It was during this high pressure run that the cover of emulator plate one was cracked. Due to the high pressure, a voltage of less than 200 volts was sufficient from this position to establish arcing to ground, and the resultant heat from this arc broke the glass cover.

After repairs to the insulation on the propellant feed line, the desired low pressure of 1.20×10^{-3} Pa was achieved and the firing run commenced at 1015 26 July 1990. This is the run from which the main body of data is drawn and with which this thesis chiefly deals. The data from both runs are presented and discussed in the next chapter.

2. Aspects of the Low Pressure Firing Run

During the main (low pressure) firing run, data were first obtained from the emulator plates at 10 to 20 volt intervals over the -200 to +200 volt range. Collecting data by hand was time consuming. Since the supply of helium was low for maintaining this pressure (due to the previous problem with the propellant feed line), the time for data collection on the reference plates was limited. In any attempt to repeat this experiment, it would be advisable to automate the data collection process.

V. RESULTS

A. CONDUCTING PLATE DATA

The main results from the low pressure run are presented in Figure 18, the nearest set of plates, through Figure 20, the furthest set of plates (see Table I). The logarithm of the current is plotted versus voltage for each plate. The readings were all taken with the arcjet firing nominally under stable vacuum pressure conditions. The chamber pressure was maintained at $1.2 \pm 0.1 \times 10^{-3}$ Pa. These graphs have the corresponding reference and emulator plates plotted on the same graph. Substantially higher electron currents than ion currents were found as expected.

As the distance between the plate and arcjet increases the current density decreases. This is expected since, as was found in previous research, the plasma density decreases as a function of distance and angle off of arcjet axis. [Refs. 6, 7, 11].

Note that in each case the emulator current density is higher and has a slightly steeper slope than the corresponding reference plate. In Figure 21 the current densities are plotted on a linear scale and this effect is more obvious. In fact the emulator current density is more than two times the current density for the reference plate at the same distance.

The ability to repeat and check readings was limited, however some spot checks were made. The electron current readings (plate at positive potential) were very

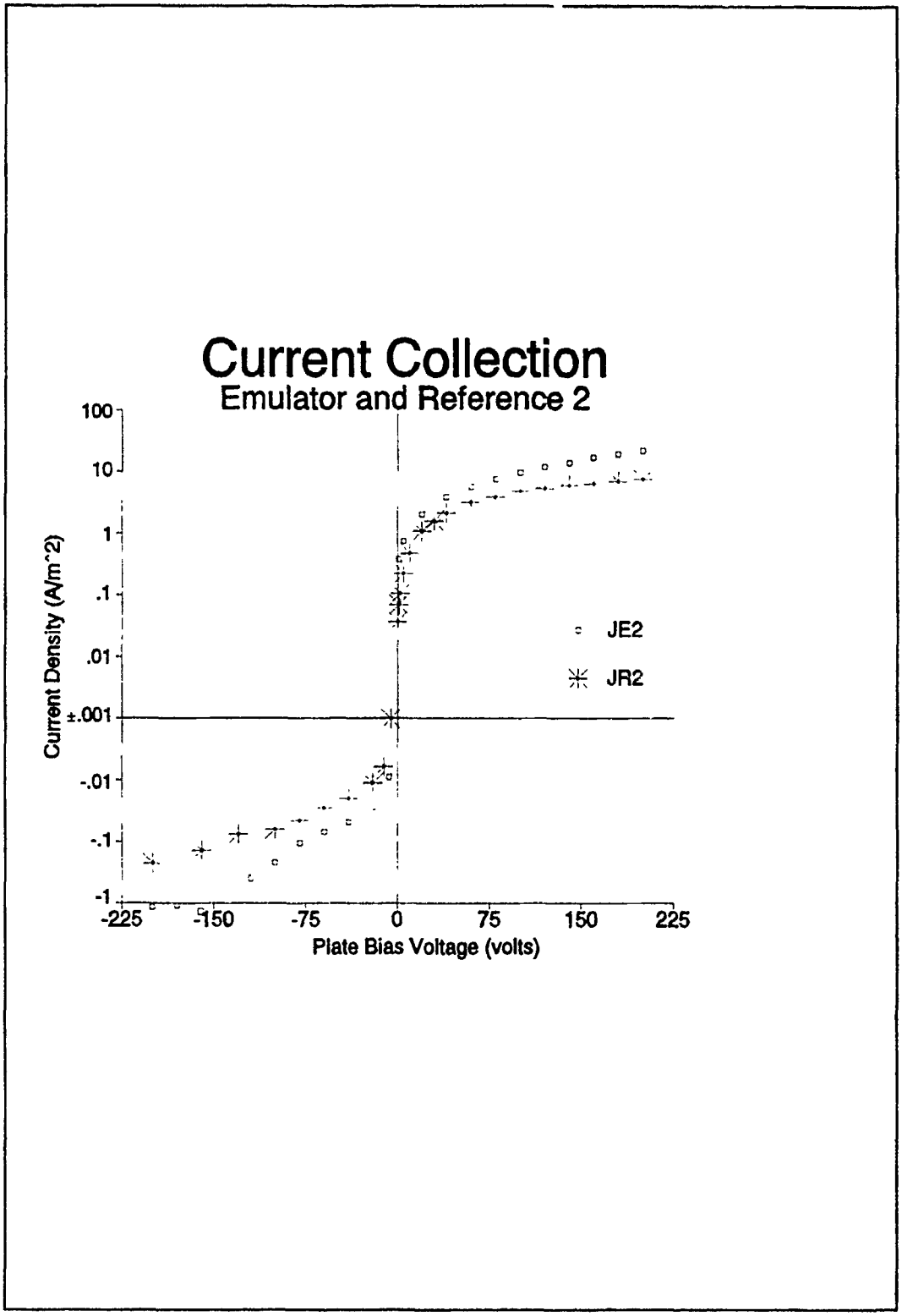

Figure 18 Emulator and Reference Plate 2 Data

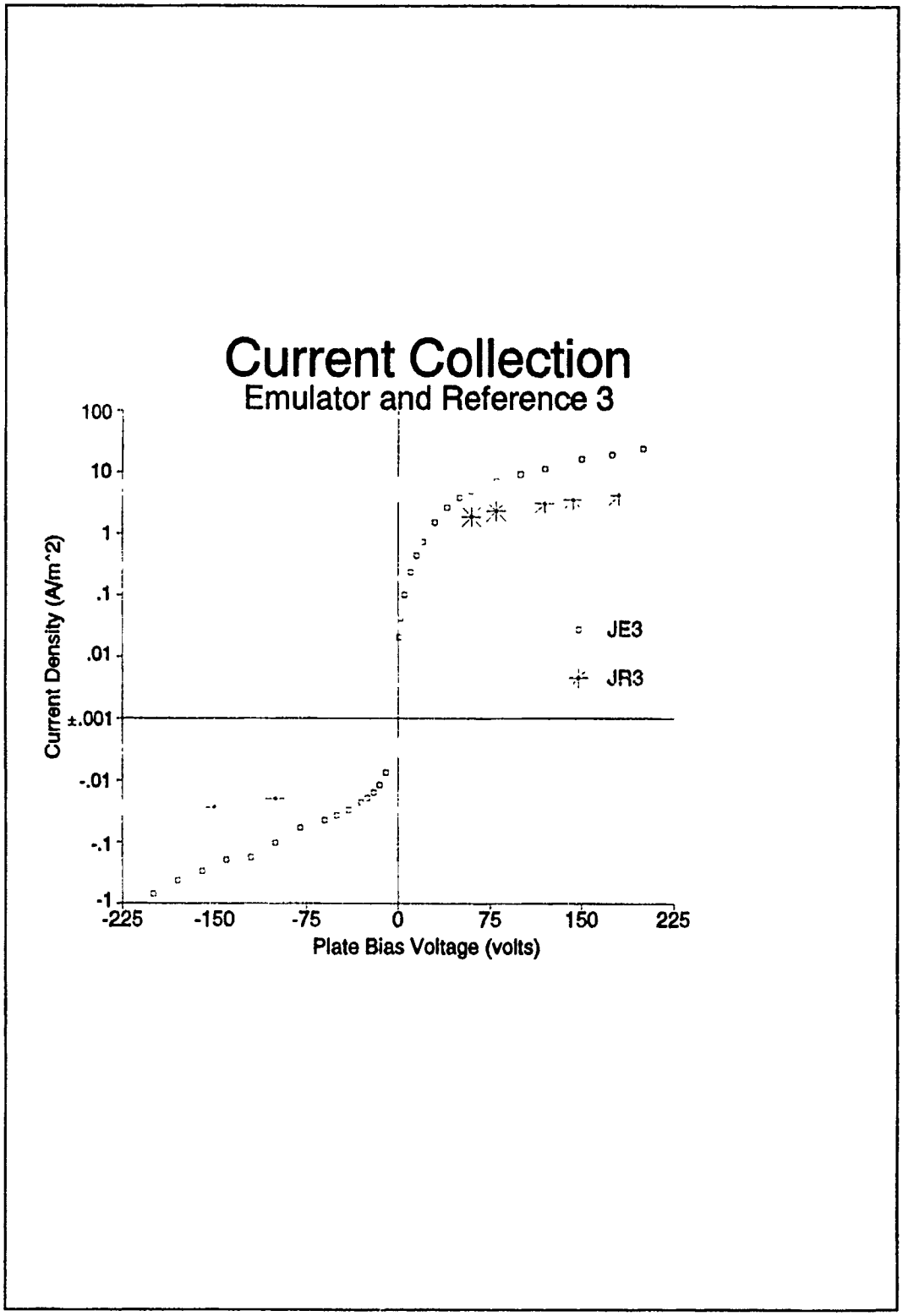

Figure 19 Emulator and Reference Plate 3 Data

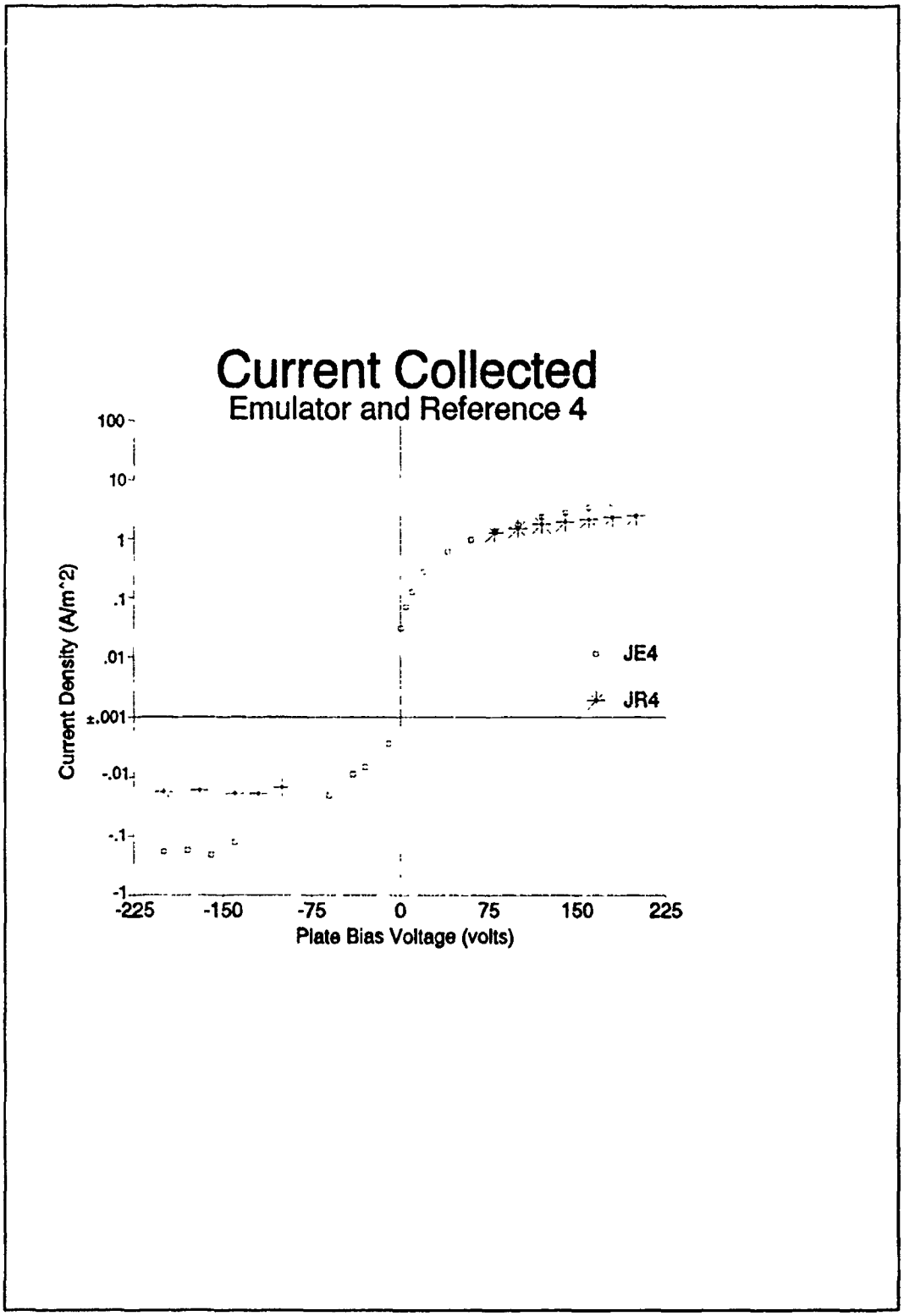

Figure 20 Emulator and Reference Plate 4 Data

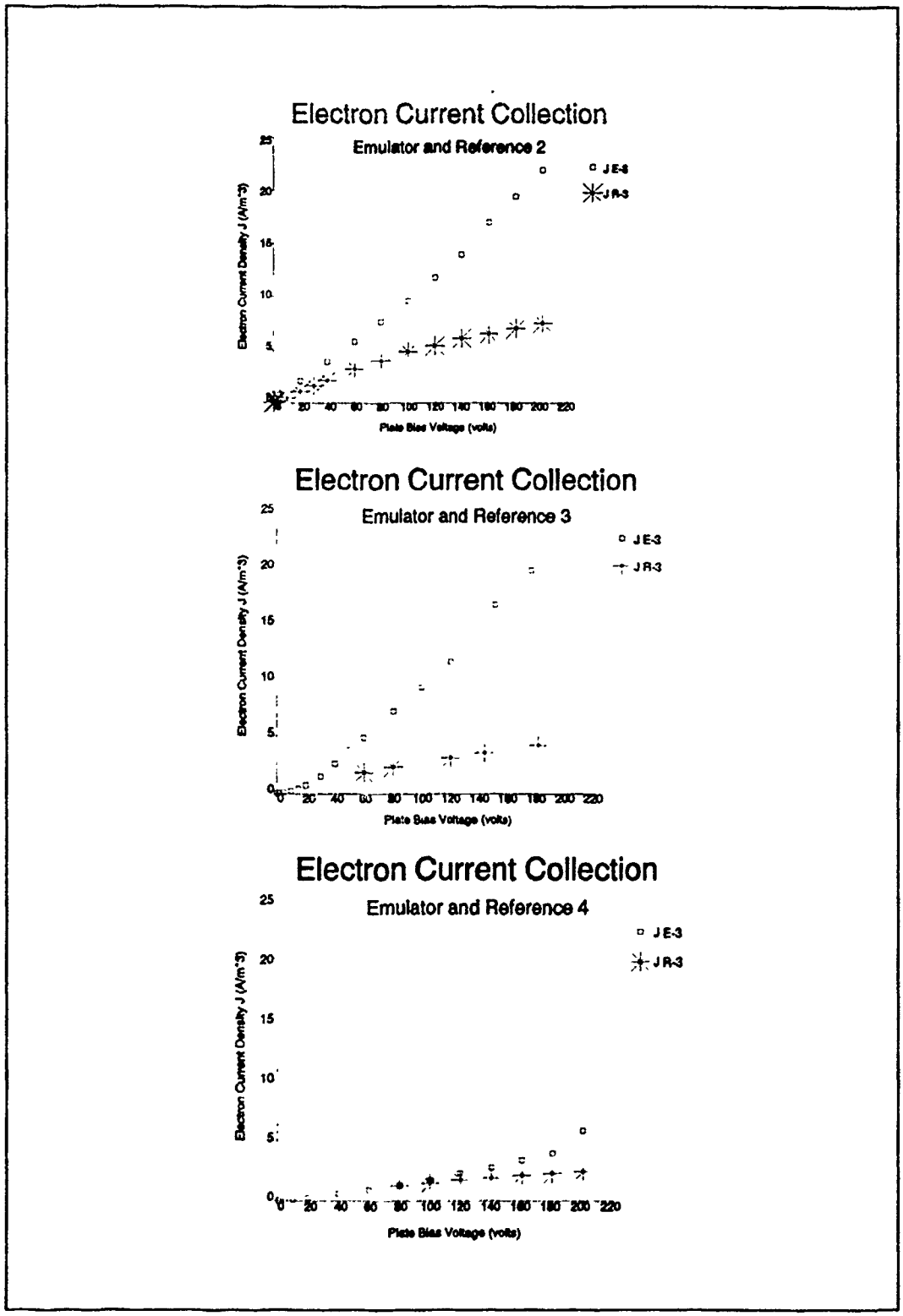

Figure 21 Linear Representation of Data

repeatable, but the ion current readings were more unstable. The error in the ion current readings is ±20% for potentials of -200 to -100 volts, and ±2% otherwise. The electron current readings are within ±0.5%.

B. HIGH PRESSURE DATA

Prior to the arcjet firing runs at 1.2×10^{-3} Pa, there was a run at a higher pressure of 15.1 Pa. During this run, data was taken on all four emulator plates. Due to the high pressure, arc breakdown was achieved at voltages somewhat below 80 volts, although this was not consistent for any position or condition. It was due to this arc breakdown that the emulator 1 coverglass was broken prior to the low pressure firing runs.

The arcjet grounding scheme allowed for the anode to be grounded to the common facility ground or left floating. During the data acquisition the grounding arrangement for the arcjet anode was switched from facility ground to the floating potential. There was a marked change in the collected currents at this point, as indicated in the graphs of this data (Figure 22 and Figure 23). After this high pressure run, the relay which allows a change in arcjet grounding configuration became inoperable and all other data were obtained with the arcjet anode at facility ground.

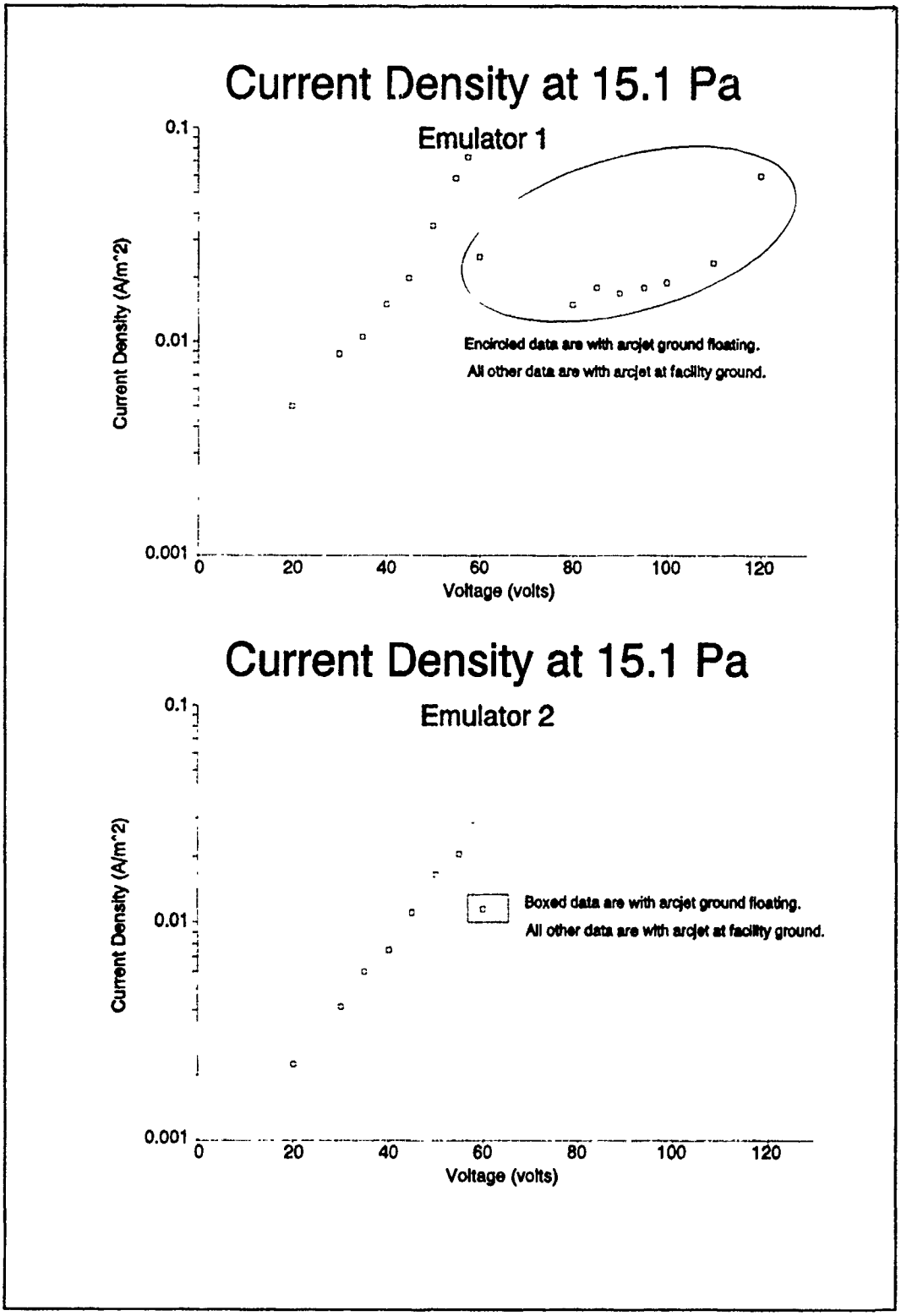

Figure 22 Emulator 1 & 2 Current Density vs. Plate Voltage Data

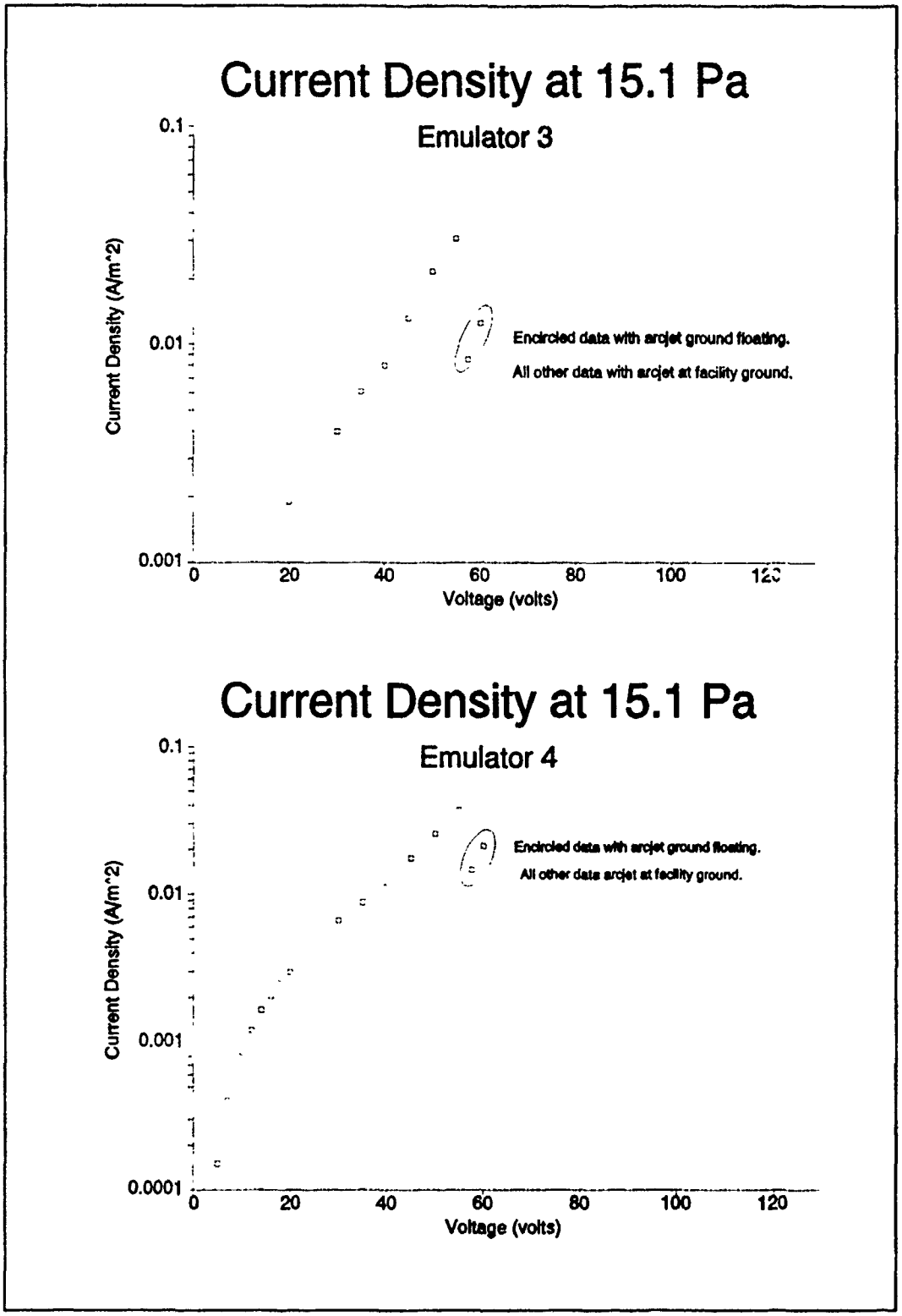

Figure 23 Emulator 3 & 4 Current Density vs. Plate Voltage Data

VI. ANALYSIS AND DISCUSSION

A. MEAN FREE PATH

In Chapter III it was pointed out that to evaluate the electron density by means of Equation 2 a large mean free path (λ) compared to other physical dimensions is required. A basic definition of λ is,

$$\lambda = \frac{1}{[n\pi d^2]} \tag{8}$$

[Refs. 11, 13]. By using the ideal gas law:

$$n = \frac{p}{kT} \tag{9}$$

we obtain

$$\lambda = \frac{kT}{p\pi d^2} \tag{10}$$

Assuming that T=5000 K and d=10^{-9} m, then λ is on the order of 20 meters. The value for T is a conservative estimate based on data from Reference 8 which has

the electron temperature average at .6 ±.1 electron volts. If the mean free path is large, then there will be little temperature decrease in the gas as it gets further from the arcjet up to the distance of the mean free path length. The value for d is a large estimate for the largest collision cross section, that of N_2. This value for λ certainly does meet the requirement as stated in Chapter III that $\lambda \gg r_p \gg \lambda_d$.

B. COLLECTED CURRENTS - DATA

A curve of J vs V as determined by Equation 3 is presented in Figure 24. This modeling of the current voltage characteristic assumes an electron/ion density, n, of 4×10^{12} m^{-3}, which is representative of the data from reference plate 2. The value used for the ion mass, m_i, is 1.1×10^{-26} kg. This value comes from the decomposed constituents of hydrazine, namely ¼ of the mass of N_2^+, ½ the mass of N^+, and 3 times the mass of H_2^+, and this value gives the best fit to the data. Figure 25 through Figure 27 compare the data from the reference plates to the modeled curve. The solid line in these figures represents the modeled curve.

The agreement of the data with the modeled curve from Equation 3 is quite good with a few exceptions. For reference plate 2 the knee in the measured electron current density is less sharp, and the measured ion current density is quite divergent from the modeled or predicted curve. The other ion and electron current densities are in excellent agreement with the model.

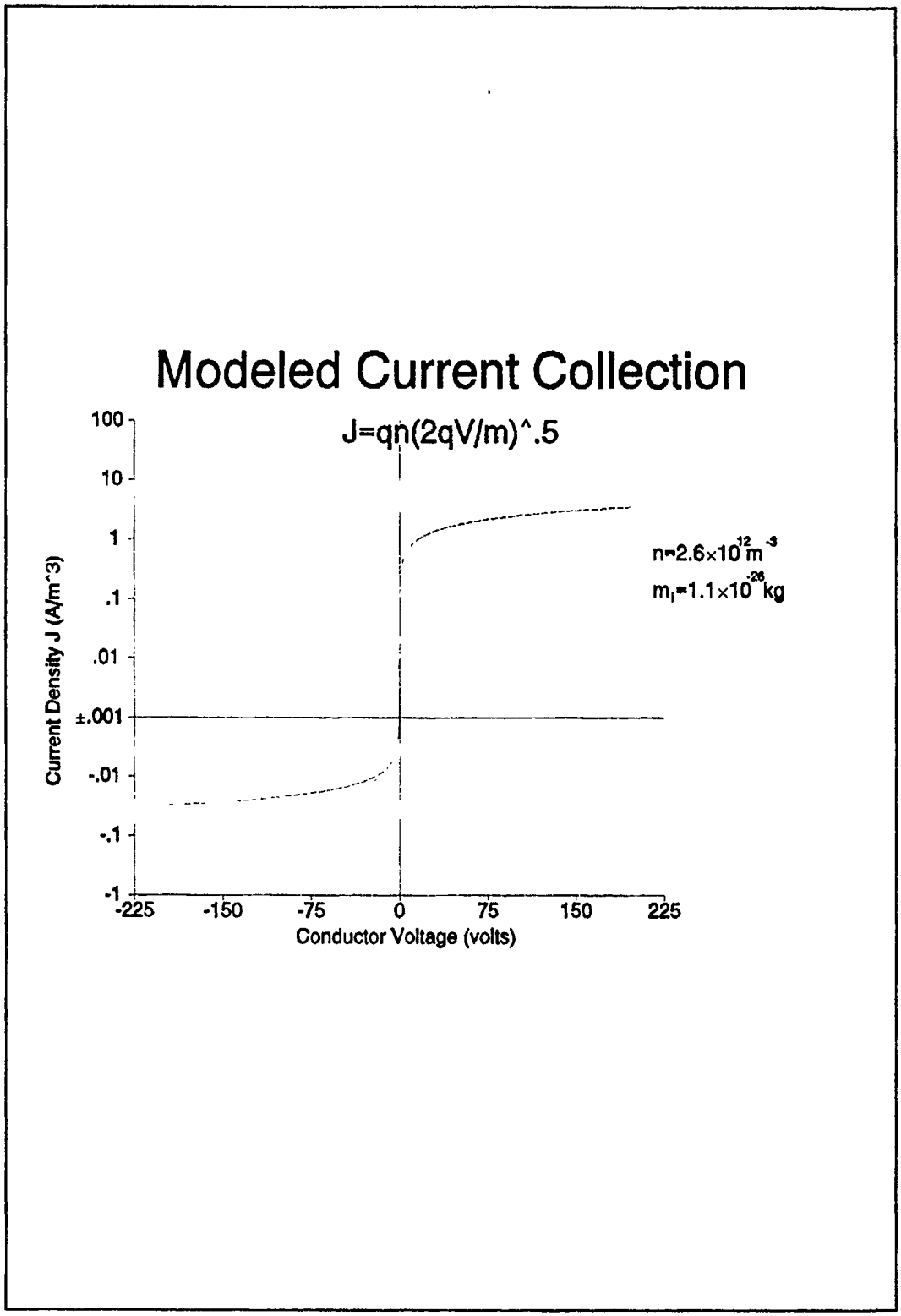

Figure 24 Plot of Current Density vs. Voltage from Equation 3

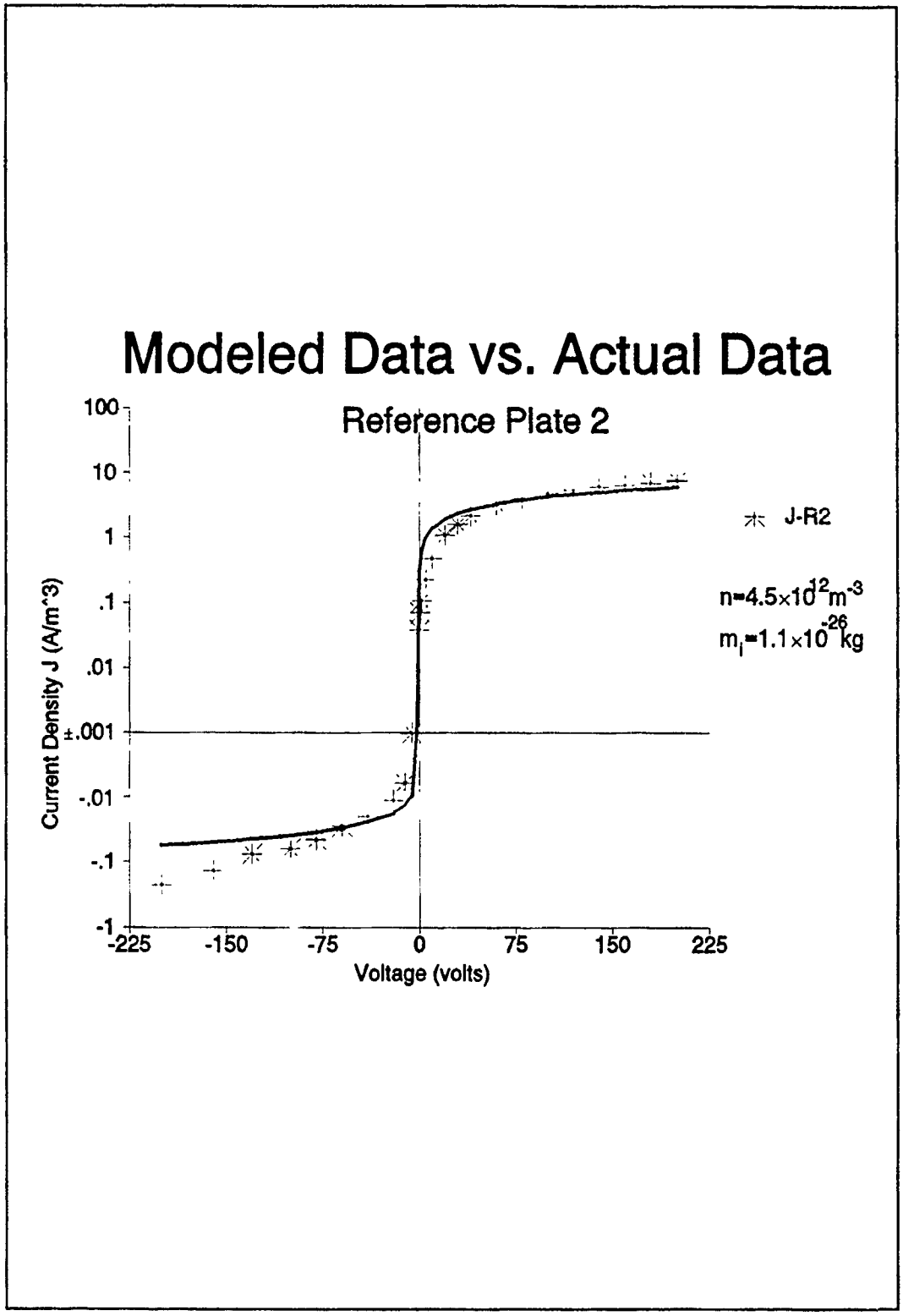

Figure 25 I-V Comparison to Model for Reference Plate 2

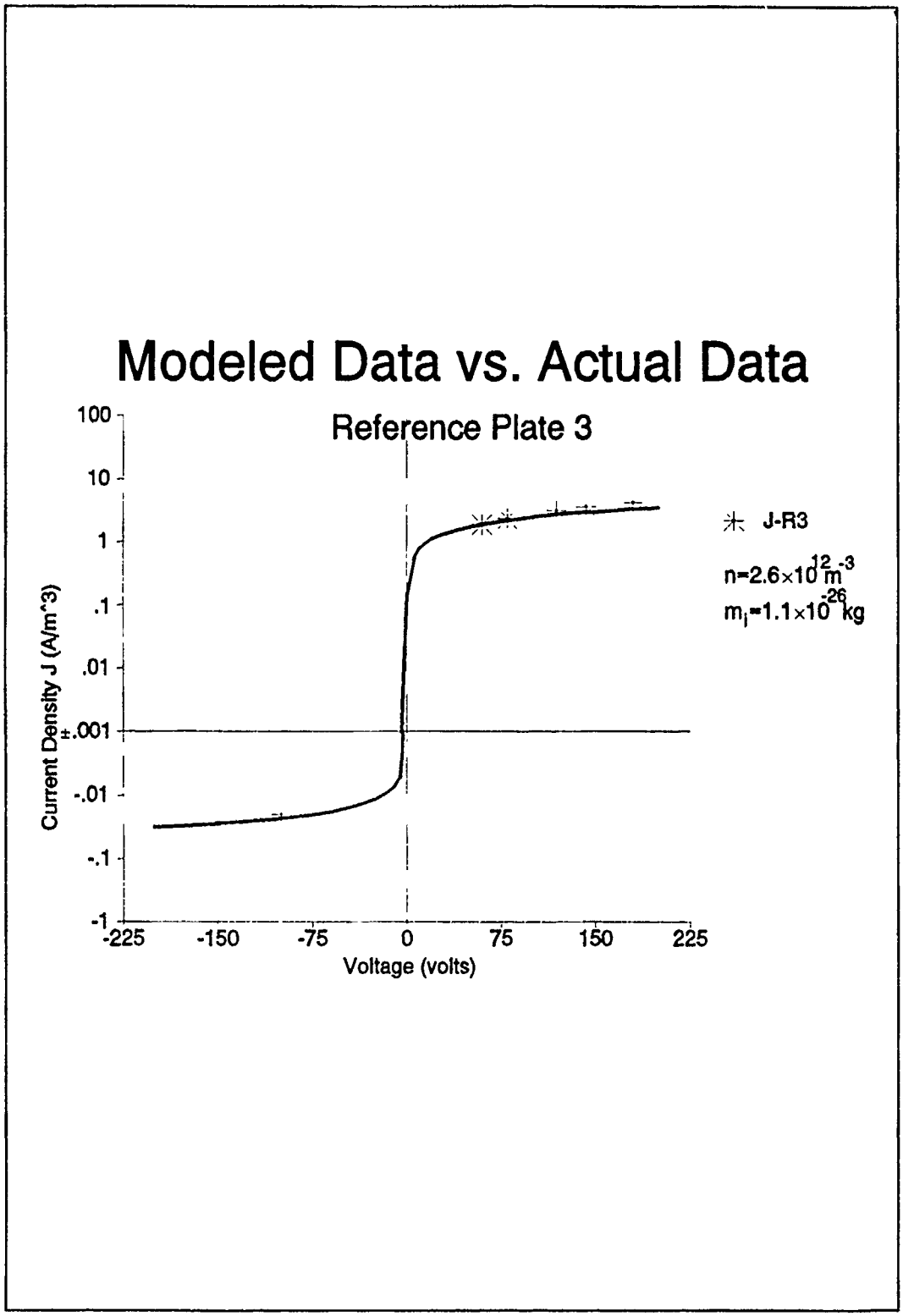

Figure 26 I-V Comparison to Model for Reference Plate 3

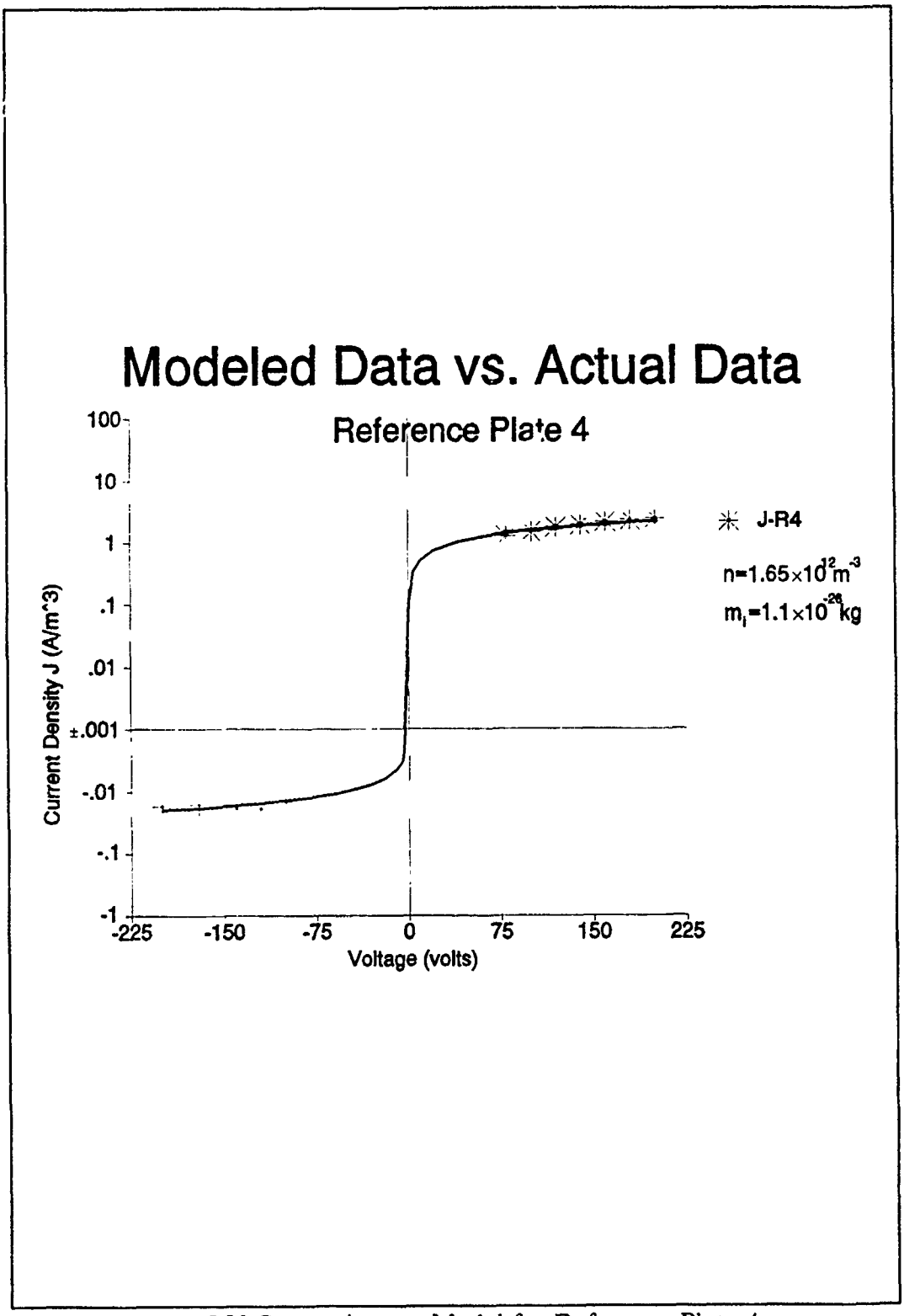

Figure 27 I-V Comparison to Model for Reference Plate 4

C. CURRENT DENSITIES

The electron densities at the plate surface are shown for each reference plate in Figure 28. The number densities are plotted versus plate bias voltage. Note the rapid increase in density at low voltage which gives way to a leveling off at higher voltages as a saturation value is approached. These number densities are derived from Equation 3, and hold for the density local to the plate.

Presented in Figure 29 is the average over the voltage of the calculated electron densities at the plate surface (from Figure 28), plotted against the distance from the arcjet exit plane. The density is approximately proportional to $r^{-3/2}$ and not r^{-3} since the density near the plate depends on the surface area of the sheath, which varies from collector to collector.

To estimate the density in the undisturbed plasma at the sheath edge, the physical process that is related to the sheath as described in Chapter III applies. The size of the sheath is characterized by the geometry of the $\phi=0$ potential surface. Initially, when the voltage is very low (near the plasma potential), the sheath boundary is very near the plate surface. As the potential is varied from the value near the plasma potential, the sheath boundary expands.

The surface area associated with this sheath boundary expands as the sheath "radius" expands (Figure 30). Radius is in quotations and is used only to relate the dimensions of this sheath. It in no way implies that it is rigidly spherical. Whatever the current collected on the plate this same current must pass through the $\phi=0$ sheath surface. If the sheath expands significantly enough, it will be more in the

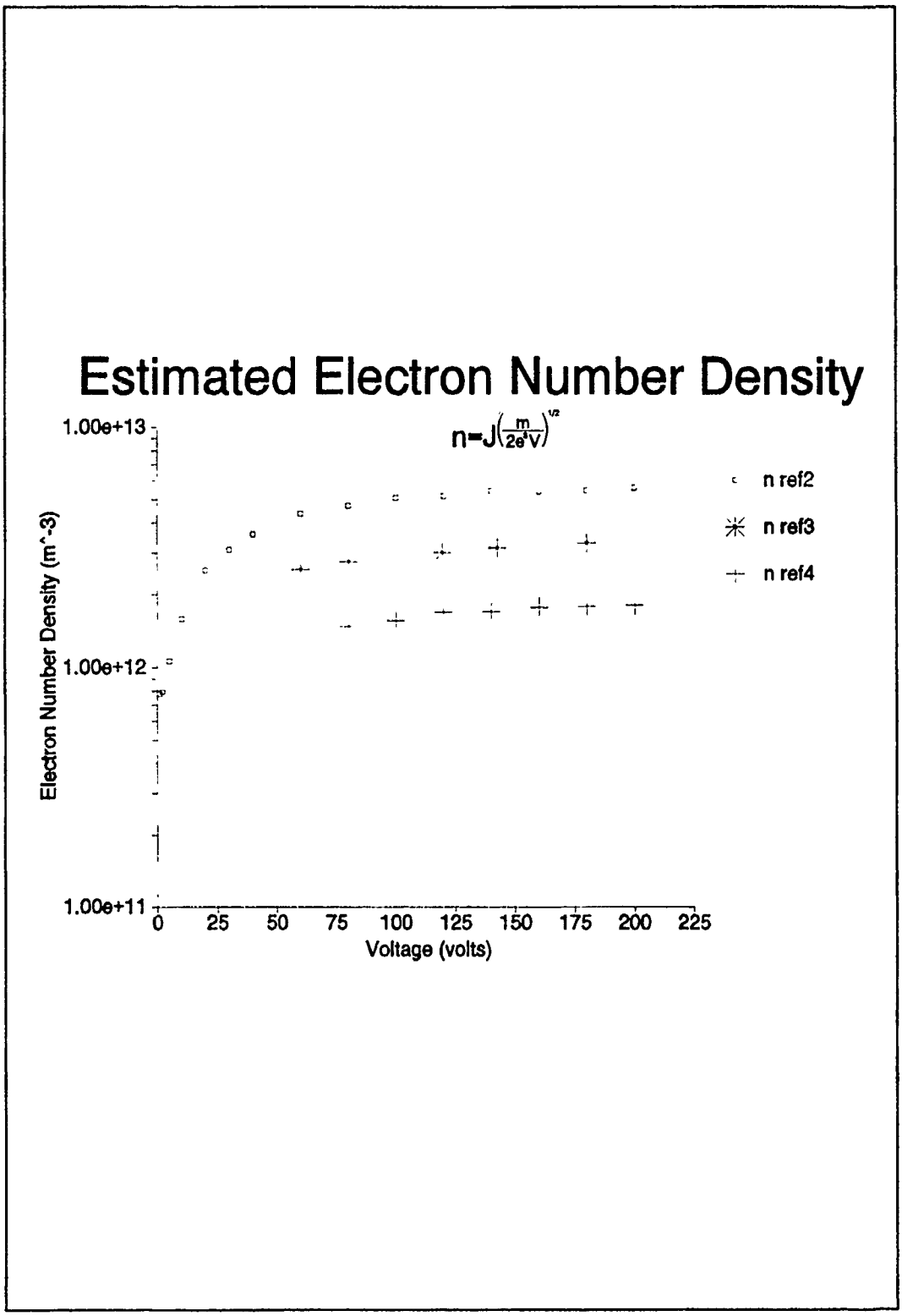

Figure 28 Electron Number Density of Reference Plates

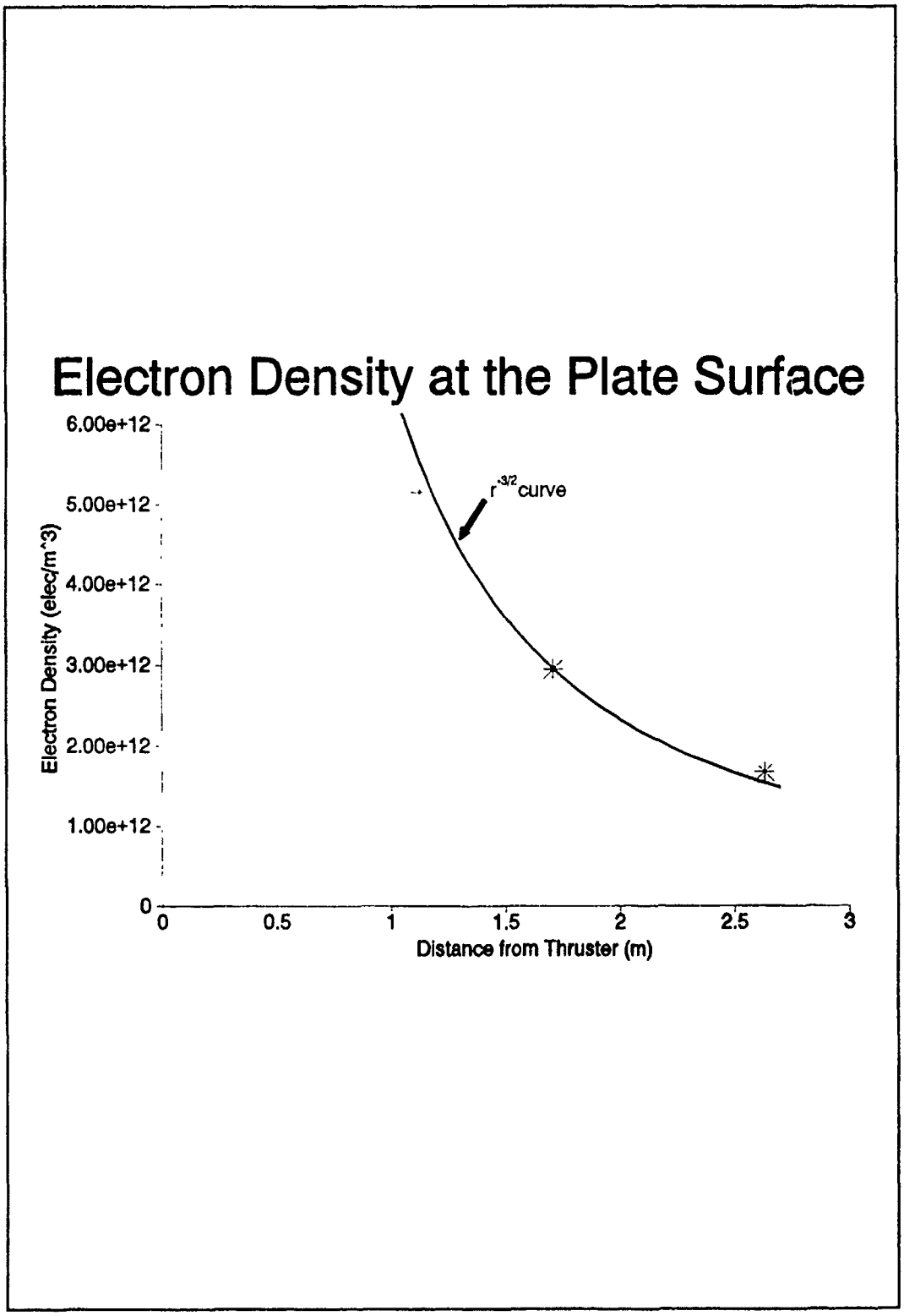

Figure 29 Electron Density as a Function of Distance

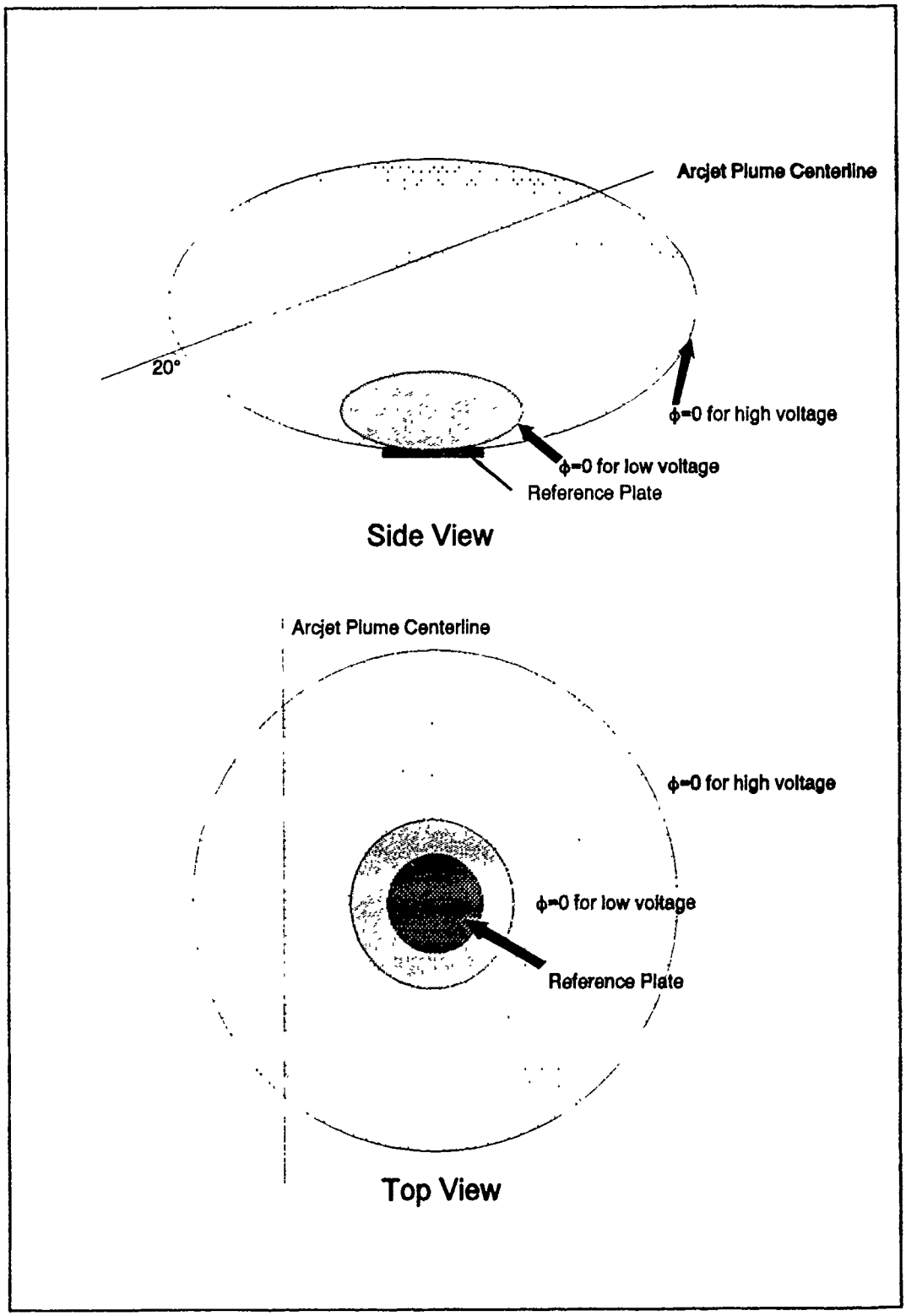

Figure 30 Sheath Geometry in Relation to Arcjet Plume Axis

arcjet plume axis for the geometry of this experiment (see Figure 30). This area has a much higher electron density [Refs. 2, 6, 11]. This will cause significantly more charged particles to pass through this sheath surface and hence be collected on the plate. This would occur if the sheath size expanded to much more than 50 cm.

If the sheath size remained less than this 50 cm size, then the increase in current collected at the plate would be related to the sheath boundary contour area. Knowing that the sheath starts out very near the plate at low voltage and assuming that it does not increase beyond the 50 cm limit at high voltage to enter the plume centerline and thus experience a huge jump in current, the electron density at the sheath edge may be estimated by

$$I=n_s eA\left(\frac{kT_e}{m}\right)^{1/2} \tag{11}$$

where n_s is the electron density at the sheath edge, and A is the area of the sheath.

From the graphs it appears that the current density is approaching some limiting or saturation value. This would indicate the sheath has stopped expanding prior to entering the plume centerline. Using this assumption, a qualitative number for n_s can be obtained. For T_e, the values of previous investigations of arcjets at this power level will suffice. The electron temperature was 0.6 $\pm$0.1 ev [Ref. 11]. Using a value of 2500 cm^2 for A and a value of 2 mA for I as found at reference plate 2, n_s is then 1.5×10^{11} m^{-3}. This compares reasonably well with the estimate from

chapter III based on extrapolation from previous work, which was a factor of ten higher.

D. ANALYSIS OF CURRENT COLLECTED BY SOLAR ARRAY

Solar arrays are constructed from individual solar cells that are connected in series strings to boost voltage. These strings are connected in parallel to boost current. Along the edge of each cell is an exposed connector strip which measures approximately 0.8 mm wide but this depends on the specific cell manufacturer. In order to estimate the effect of this plume on a solar panel in this configuration, the following method with its assumptions and approximations was used.

A silicon type solar array of 750 watts would have two panels of very nearly the same size as the panel in this experiment [Ref. 14]. The voltage on the exposed connector strips would vary from zero volts, at the first set near the spacecraft body, to 25.7 volts, at the outer edge of the array. The increase at each series connection would be 0.367 volts. The length of each 0.8 mm wide connector strip would be 124 cm across the panel. To determine the power lost at each step or connector strip, the panel is divided into thirds so that an emulator from this experiment would be centered in each third. The current density values measured for the respective emulator are applied to the exposed connector strip areas. The current density is linearly interpolated between the measured voltages and applied for the voltage of each strip. The current density J_n of each strip is found by

$$J_n = J_{m2} - \left[\frac{(V_{m2} - V_n)}{(V_{m2} - V_{m1})} (J_{m2} - J_{m1}) \right] \quad (12)$$

where subscripts m1 and m2 indicate the measured values of J and V for the appropriate emulator that bracket the connector strip's actual voltage V_n. J_n is then multiplied by the area and the voltage at each strip to determine power lost. Finally, all the connector strip power values are summed to determine the power lost due to the arcjet plume. The loss in this example is 0.39 watts of the 375 watts produced by the panel. The whole array (both panels) produce 750 watts so the power loss percentage in this example is 0.05%.

VII. CONCLUSIONS

A. SOLAR ARRAY PERFORMANCE

The use of arcjets should cause very little degradation to solar arrays due to the power loss of 0.05%, as estimated in this experiment. This was only for one arcjet/array configuration. If the angle between arcjet and solar array surface is significantly lessened, then the power losses may be much higher. With the array surface more directly in the arcjet plume the currents collected would jump significantly. This would be for very limited configurations and can be avoided during the design of the spacecraft.

B. FURTHER RESEARCH

Investigation of the far-field-arcjet plume is a natural follow up to this preliminary look at the effects of this slightly ionized plume. Knowing the electron density as a function of angle and range within the plume would facilitate calculations of the power losses for any given firing configuration with respect to the array surfaces.

LIST OF REFERENCES

1. Rocket Research Company, Report 90-H-1478, *Electric Propulsion Technology Status*, by W. W. Smith and R. J. Cassidy, August 1990.

2. NASA CR-54691, *Study of Arcjet Propulsion Devices*, by W. M. Van Camp, et. al., March 1966.

3. Giannini Scientific Corporation, APL-TDR-64-58, *30 kW Arc-Jet Thruster Research*, by J. P. Todd, March 1964.

4. NASA CR-54035, *Research and Advanced Development of a 2 kW Arc-Jet Thruster*, by O. J. McCaughey, et. al., 1963.

5. Institut für Raumfahrtsysteme, Universität Stuttgart, Report 88-107, *A 15 kW Experimental Arcjet*, by H. L. Kurtz, et. al., 1988.

6. NASA TM-89924, *Langmuir Probe Surveys of an Arcjet Exhaust*, by L. M. Zana, July 1987.

7. NASA TM-103241, *Preliminary Plume Characteristics of an Arcjet Thruster*, by D. H. Manzella, et. al., July 1990.

8. NASA TM-102284, *The Effects of Arcjet Operating Condition and Constrictor Geometry on the Plasma Plume*, by L. M. Carney and J. M. Sankovic, July 1989.

9. L. Schott, *Electric Probes*, Plasma Diagnostics, edited by W. Lochte-Holtgreven, North-Holland Publishing Co., 1968.

10. F. F. Chen, *Electric Probes*, Plasma Diagnostic Techniques, edited by R. H. Huddleston and S. L. Leonard, Academic Press, 1965.

11. NASA TM-100258, *An Experimental Investigation of an Arcjet Thruster Exhaust Using Langmuir Probes*, by L. M. Carney, April 1988.

12. TRW Inc., Test Plan No. 54732-6004-UT-00, *Test Plan, Arcjet System Integration Development Program*, by R. J. Glumb, 13 April 1990.

13. F. F. Chen, *Introduction to Plasma Physics and Controlled Fusion*, 2d ed., v. 2, Plenum Publishing Corporation, 1980.

14. B. N. Agrawal, *Design of Geosynchronous Spacecraft*, Prentice-Hall Inc., New Jersey, 1986.

INITIAL DISTRIBUTION LIST

1.	Defense Technical Information Center Cameron Station Alexandria, Virginia 22304-6145	2
2.	Superintendent Attn: Library, Code 52 Naval Postgraduate School Monterey, California 93943-5002	2
3.	Sidney Zafran TRW Applied Technology Division, Space & Technology Group Building 01, Room 2260, One Space Park Redondo Beach, California 90278	1
4.	Charlie Vaughn Rocket Research Company, Electric Propulsion Division 11441 Willows Road NE Redmond, Washington 98073	1
5.	Superintendent Attn: Oscar Biblarz, Code AA/Bi Naval Postgraduate School Monterey, California 93943-5002	1
6.	Superintendent Attn: R. C. Olsen, Code PH/Os Naval Postgraduate School Monterey, California 93943-5002	1
7.	Superintendent Physics Department, Code PH Naval Postgraduate School Monterey, California 93943-5002	1
8.	Superintendent Attn: B. N. Agrawal, Code AA/Ag Naval Postgraduate School Monterey, California 93943-5002	1

9. Francis M. Curran — 1
NASA Lewis Research Center
21000 Brookpark Road
Cleveland, Ohio 44135

10. Dr. Dale Ferguson, MS 302-1 — 1
NASA Lewis Research Center
21000 Brookpark Road
Cleveland, Ohio 44135

11. Norman Grier, MS 302-1 — 1
NASA Lewis Research Center
21000 Brookpark Road
Cleveland, Ohio 44135

12. Dr. Paul Wilbur — 1
Department of Mechanical Engineering
Colorado State University
Fort Collins, Colorado 80523

13. Dr. R. G. Joiner — 1
Office of Naval Research, Code 1114 SP
800 North Quincy Street
Arlington, Virginia 22217-5000